

PARTITIONED CONSERVATIVE, VARIABLE STEP, SECOND-ORDER METHOD FOR MAGNETO-HYDRODYNAMICS IN ELSÄSSER VARIABLES

ZHEN YAO*, CATALIN TRENCEA†, AND WENLONG PEI‡

Abstract. Magnetohydrodynamics (MHD) describes the interaction between electrically conducting fluids and electromagnetic fields. We propose and analyze a symplectic, second-order algorithm for the evolutionary MHD system in Elsässer variables. We reduce the computational cost of the iterative non-linear solver, at each time step, by partitioning the coupled system into two sub-problems of half size, solved in parallel. We prove that the iterations converge linearly, under a time step restriction similar to the one required in the full space-time error analysis. The variable step algorithm unconditionally conserves the energy, cross-helicity and magnetic helicity, and numerical solutions are second-order accurate in the L^2 and H^1 -norms. The time adaptive mechanism, based on a local truncation error criterion, helps the variable step algorithm balance accuracy and time efficiency. Several numerical tests support the theoretical findings and verify the advantage of time adaptivity.

Key words. Magnetohydrodynamics, Elsässer variables, partitioned algorithms, iterative methods, second-order accurate, variable steps, time adaptivity

AMS subject classifications. 76W05, 65M12, 65M60, 35Q30, 35Q61

1. Introduction. The equations of magnetohydrodynamics [1] (MHD) describe the motion of electrically conducting, incompressible flows in the presence of magnetic fields. The understanding of the MHD system is essential to numerous applications in science and engineering, astrophysics [4, 16, 35], geophysics [14, 36], sea water propulsion [31], cooling system design [3, 23] and process metallurgy [12]. Given a bounded domain $\Omega \subset \mathbb{R}^d$ ($d = 2, 3$) and time interval $[0, T]$, the fluid velocity field u , magnetic field B and the pressure p satisfy

$$\partial_t u + (u \cdot \nabla)u - (B \cdot \nabla)B - \nu \Delta u + \nabla p = f, \quad \nabla \cdot u = 0, \quad (1.1)$$

$$\partial_t B + (u \cdot \nabla)B - (B \cdot \nabla)u - \nu_m \Delta B = 0, \quad \nabla \cdot B = 0, \quad (1.2)$$

with Dirichlet boundary conditions: $u|_{\partial\Omega} = 0$, $B|_{\partial\Omega} = B_o$. Here ν is the kinematic viscosity, ν_m is the magnetic resistivity, B_o is a constant external magnetic field, and f is an external force. The MHD flows entail two distinct physical processes: the motion of fluid - governed by the hydrodynamics equations (1.1), and its interaction with the magnetic fields - governed by the Maxwell equations (1.2). Splitting the magnetic field B into its mean and fluctuation $B = B_o + b$, the Elsässer variables [15]

$$z^+ = u + b, \quad z^- = u - b,$$

merge the physical properties of the Navier-Stokes and Maxwell equations. The Elsässer variables, used in plasma turbulence, differentiate between the MHD waves

*Department of Mathematics, University of Pittsburgh, Pittsburgh, PA 15260, USA. Email: zhy@pitt.edu.

†Department of Mathematics, University of Pittsburgh, Pittsburgh, PA 15260, USA. Email: trenchea@pitt.edu.

‡Department of Mathematics, The Ohio State University, Columbus, OH 43210, USA. Email: pei.176@osu.edu.

propagating parallel or anti-parallel to the main magnetic field B_o . The MHD equations (1.1)-(1.2) are equivalently written in terms of the Elsässer variables as

$$\begin{cases} \partial_t z^\pm \mp (B_o \cdot \nabla) z^\pm + (z^\mp \cdot \nabla) z^\pm - \nu^+ \Delta z^\pm - \nu^- \Delta z^\mp + \nabla p = f, \\ \nabla \cdot z^\pm = 0, \end{cases} \quad (1.3)$$

and $z^\pm = 0$ on $\partial\Omega$. Here $\nu^+ = (\nu + \nu_m)/2$ and $\nu^- = (\nu - \nu_m)/2$. The nonlinear interactions between the Alfvénic fluctuations z^\pm , via the cross-coupling term $(z^\mp \cdot \nabla) z^\pm$, are the basis of the Alfvén effect, a fundamental interaction process [13, 18, 21, 26].

The numerical simulation of the fully-coupled system (1.3) is computationally challenging. The monolithic methods or implicit fully-coupled algorithms in the u, B variables [41], which assemble the coupled system at each time step and solve it iteratively, are stable and accurate, but quite demanding in computational speed and storage.

The implicit-explicit (IMEX) partitioned methods [30, 39], at each time step, decouple the computations and treat the subphysics/subdomain variables implicitly in time, while the coupling terms are evaluated explicitly in time (by lagging or extrapolating values), hence solving two subproblems in parallel. The IMEX decoupling highly reduces the computational complexity, but often introduces a Lyapunov-type instability.

Inhere we propose an algorithm which, at each time step, partitions the computations via an iterative process, and prove that the iterations linearly converge to the solution of the fully-coupled implicit monolithic method. The fully-coupled implicit monolithic method is the variable step, one-step, second-order, symplectic, midpoint method.

Given z_n^\pm at time t_n , the fully-coupled scheme solves for z^\pm at time t_{n+1} by

$$\begin{cases} \frac{z_{n+1}^\pm - z_n^\pm}{\tau_n} \mp (B_o \cdot \nabla) z_{n+1/2}^\pm + (z_{n+1/2}^\mp \cdot \nabla) z_{n+1/2}^\pm \\ - \nu^+ \Delta z_{n+1/2}^\pm - \nu^- \Delta z_{n+1/2}^\mp + \nabla p_{n+1/2}^\pm = f(t_{n+1/2}), \\ \nabla \cdot z_{n+1/2}^\pm = 0, \end{cases} \quad (1.4)$$

where $t_{n+1/2} = (t_{n+1} + t_n)/2$, $\tau_n = t_{n+1} - t_n$ is the local time step, and $z_{n+1/2}^\pm, p_{n+1/2}^\pm$ approximate z^\pm, p at $t_{n+1/2}$, respectively. The implementation of the midpoint method (1.4) can be simplified by refactorization into a backward Euler (BE) solve on the first half-interval, and a linear extrapolation (post-process):

Step 1. BE solver for $z_{n+1/2}^\pm$ on $[t_n, t_{n+1/2}]$

$$\begin{cases} \frac{z_{n+1/2}^\pm - z_n^\pm}{\tau_n/2} \mp (B_o \cdot \nabla) z_{n+1/2}^\pm + (z_{n+1/2}^\mp \cdot \nabla) z_{n+1/2}^\pm \\ - \nu^+ \Delta z_{n+1/2}^\pm - \nu^- \Delta z_{n+1/2}^\mp + \nabla p_{n+1/2}^\pm = f(t_{n+1/2}), \\ \nabla \cdot z_{n+1/2}^\pm = 0. \end{cases} \quad (1.5)$$

Step 2. Post-process for z_{n+1}^\pm : $z_{n+1}^\pm = 2z_{n+1/2}^\pm - z_n^\pm$.

The post-process is equivalent to the forward Euler (FE) solver on $[t_{n+1/2}, t_{n+1}]$ [8].

We decouple the implicit monolithic midpoint method (1.4) by partitioning via iterations in the refactorized implicit BE solver (1.5) for $z_{n+1/2}^\pm$. With an initial guess

$z_{(0)}^\pm = \frac{3}{2}z_n^\pm - \frac{1}{2}z_{n-1}^\pm$, we seek $z_{(k)}^\pm$ and $p_{(k)}$ such that

$$\begin{cases} \frac{z_{(k)}^\pm - z_n^\pm}{\tau_n/2} \mp (B_\circ \cdot \nabla) z_{(k)}^\pm + (z_{(k-1)}^\mp \cdot \nabla) z_{(k)}^\pm \\ - \nu^+ \Delta z_{(k)}^\pm - \nu^- \Delta z_{(k-1)}^\mp + \nabla p_{(k)}^\pm = f(t_{n+1/2}), \\ \nabla \cdot z_{(k)}^\pm = 0. \end{cases} \quad (1.6)$$

In Theorem 3.1 we prove that the sequence $\{z_{(k)}^\pm\}_{k=0}^\infty$ in the BE partitioned iteration (1.6) converges linearly to $z_{n+1/2}^\pm$, strongly in $H^1(\Omega)$, provided the time step τ_n is small enough. The BE partitioned iteration (1.6) is computationally efficient [38], as it decouples the cross-coupling terms $(z^\mp \cdot \nabla) z^\pm$. Due to the fact that the symplectic, second-order accurate, one-step implicit midpoint method conserves all quadratic Hamiltonians [2, 5, 8], the algorithm (1.4) conserves

- the model energy: $\mathcal{E}(t) = \frac{1}{2} \int_\Omega (|u|^2 + |B|^2) dx$,
- the cross-helicity: $\mathcal{H}_C(t) = \frac{1}{2} \int_\Omega u \cdot B dx$,
- the magnetic-helicity: $\mathcal{H}_M(t) = \frac{1}{2} \int_\Omega \mathbb{A} \cdot B dx$ for the vector potential \mathbb{A} such that $B = \nabla \times \mathbb{A}$,

and its numerical solutions are second-order accurate in time. The midpoint rule is a special member of the robust Dahlquist-Liniger-Nevanlinna (DLN) family of one-leg second-order variable step methods [11, 27–29, 33], which are unconditionally stable for any arbitrary sequence of time steps. Also having the smallest error constant in the DLN family makes the midpoint method an ideal choice for time adaptivity, based on various criteria (minimum numerical dissipation, global error or local truncation error (LTE)). Time adaptivity is an effective approach which balances computational costs and accuracy in the simulation of many stiff ordinary differential equations and fluid models [9, 27, 29, 33, 34, 37]. Here we utilize the explicit AB2-like method (a variant of the two-step Adams-Bashforth method [8]) to estimate the LTE of the algorithm (1.4), with negligible extra computational costs. This adaptive mechanism achieves outstanding performance in numerous highly stiff evolutionary equations [7] and thus deserves a fair trial in the simulations of MHD flows.

The rest of report is organized as follows. In Section 2 we give some necessary notations and preliminary results. In Section 3 we present detailed numerical analysis of the implicit fully-decoupled algorithm (1.4) with the partitioned BE iterations (1.6). In subsection 3.1 we prove that the sequence $\{z_{(k)}^\pm\}_{k=0}^\infty$ in (1.6) converges linearly to $z_{n+1/2}^\pm$ in (1.5), strongly in $H^1(\Omega)$. We show in subsection 3.2 that the implicit algorithm (1.4) is unconditionally stable, and (in the ideal case) conserves the quadratic Hamiltonians: energy, cross-helicity and magnetic-helicity. The variable step error analysis for the Elsässer variables z^\pm is provided in subsection 3.4. Several numerical tests are presented in Section 5 to support main results of the report. We verify that the algorithm (1.4)-(1.6) is second-order accurate and conserves over long time the model energy, the cross-helicity and the magnetic-helicity, on the two-dimensional travelling wave problem [40], and Hartmann flows [19].

The efficiency of time adaptivity using a LTE criterion is confirmed on these two examples, endowed with a Lindberg type time component [32].

2. Preliminaries and Notations. Let $\Omega \subset \mathbb{R}^d$ ($d=2,3$) be a bounded domain, and denote by $L^p(\Omega)$ the Banach space of Lebesgue measurable function f such that $|f|^p$ is integrable. We denote by $H^\ell(\Omega)$ is the usual Sobolev space $W^{\ell,2}(\Omega)$ with norm $\|\cdot\|_\ell$ and semi-norm $|\cdot|_\ell$. In the case $\ell=0$, $H^0(\Omega)$ reduces to the $L^2(\Omega)$ Hilbert space, with norm $\|\cdot\|$ and inner product (\cdot, \cdot) . The function spaces X for Elsässer variables z^\pm and Q for pressure p are

$$X = (H_0^1(\Omega))^d = \left\{ v \in (H^1(\Omega))^d : v|_{\partial\Omega} = 0 \right\}, \quad Q = \left\{ q \in L^2(\Omega) : (q, 1) = 0 \right\}.$$

The divergence-free space for X is

$$V = \left\{ v \in X : (\nabla \cdot v, q) = 0, \quad \forall q \in Q \right\},$$

and let X' denote the dual space of X with the dual norm

$$\|f\|_{-1} := \sup_{v \in X, v \neq 0} \frac{(f, v)}{\|\nabla v\|}, \quad \forall f \in X'. \quad (2.1)$$

For spatial discretization we use the finite element method. Let $\{\mathcal{T}_h\}$ be a family of edge-to-edge triangulation with diameter $h \in (0,1)$. We denote $X^h \subset X$ and $Q^h \subset Q$ as certain finite element spaces for Elsässer variables z^\pm and pressure p respectively. The divergence-free space for X^h is

$$V^h := \left\{ v^h \in X^h : (q^h, \nabla \cdot v^h) = 0, \quad \forall q^h \in Q^h \right\}.$$

We assume that X^h is the C^m -space containing polynomials of highest degree r , Q^h is the C^m -space containing polynomials of highest degree s , and we have the following approximations for $v \in (H^{r+1})^d \cap X$ and $q \in H^{s+1} \cap Q$

$$\begin{aligned} \inf_{v^h \in X^h} \|v - v^h\|_{\ell_1} &\leq C_A^{\ell_1, r} h^{r+1-\ell_1} |v|_{r+1}, \quad 0 \leq \ell_1 \leq \min\{m+1, r+1\}, \\ \inf_{q^h \in Q^h} \|q - q^h\|_{\ell_2} &\leq C_A^{\ell_2, s} h^{s+1-\ell_2} |q|_{s+1}, \quad 0 \leq \ell_2 \leq \min\{m+1, s+1\}, \end{aligned} \quad (2.2)$$

where the constants $C_A^{\ell_1, r}, C_A^{\ell_2, s} > 0$ are independent of h (see e.g., [6, 10]). We also recall the inverse inequality for X^h is

$$|v^h|_1 \leq C_I h^{-1} \|v^h\|, \quad \forall v^h \in X^h. \quad (2.3)$$

for $C_I > 0$ independent of h . To ensure the robustness of the fully discrete algorithm, we assume that X^h and Q^h satisfy the discrete inf-sup condition (Ladyzhenskaya-Babuška-Brezzi condition)

$$\inf_{q^h \in Q^h} \sup_{v^h \in X^h} \frac{(\nabla \cdot v^h, q^h)}{\|\nabla v^h\| \|q^h\|} \geq \beta_{\text{is}} > 0, \quad (2.4)$$

where β_{is} is independent of h . The Taylor-Hood ($\mathbb{P}2\text{-}\mathbb{P}1$) space and the Mini element space are typical examples meeting this criterion. For any pair $(u, p) \in V \times Q$, the Stokes projection $(I_{\text{St}} u, I_{\text{St}} p) \in V^h \times Q^h$ is defined to be the unique solution to the following Stokes problem

$$\begin{cases} (\nabla u - \nabla I_{\text{St}} u, \nabla v^h) = (p - I_{\text{St}} p, \nabla \cdot v^h) \\ -(q^h, \nabla \cdot I_{\text{St}} u) = 0 \end{cases}, \quad \forall (v^h, q^h) \in X^h \times Q^h. \quad (2.5)$$

We recall that if the pair (X^h, Q^h) satisfies the discrete inf-sup condition in (2.4), the following approximation property of the Stokes projection [20, 25] holds

$$|u - I_{\text{St}} u|_1 \leq 2 \left(1 + \frac{1}{\beta_{\text{is}}}\right) \inf_{v^h \in X^h} |u - v^h|_1 + \inf_{q^h \in Q^h} \|p - q^h\|. \quad (2.6)$$

In the error analysis we will make use of the skew-symmetric nonlinear operator

$$\mathcal{N}(u, v, w) = \frac{1}{2}(u \cdot \nabla v, w) - \frac{1}{2}(u \cdot \nabla w, v), \quad \forall u, v, w \in (H^1(\Omega))^d, \quad (2.7)$$

which can also be written as

$$\mathcal{N}(u, v, w) = (u \cdot \nabla v, w) + \frac{1}{2}((\nabla \cdot u)v, w), \quad \forall u, v, w \in X. \quad (2.8)$$

Finally, we recall the following Sobolev embedding and Ladyzhenskaya inequality [17, p. 52]

$$\|u\|_{L^3(\Omega)} \leq \left(\frac{1}{d^{1/2}}\right)^{d/6} \|u\|^{1-d/6} \|\nabla u\|^{d/6}, \quad (2.9)$$

$$\|u\|_{L^4(\Omega)} \leq \left(\frac{2(d-1)}{d^{3/2}}\right)^{d/4} \|u\|^{1-d/4} \|\nabla u\|^{d/4}, \quad \forall u \in (H^1(\Omega))^d. \quad (2.10)$$

3. Partitioned, conservative, variable step, second-order method. In this section, first we prove the linear convergence of the iterative solution of the partitioned method (1.6), to the solution at time $t_{n+1/2}$ of the fully coupled midpoint method (1.4). Secondly, we prove the stability of (1.4), and the conservation of three quadratic invariants: the energy in the original variables u and B , the cross-helicity and the magnetic-helicity. Finally, we perform error analysis of the full time-space discretization, using the finite element method.

3.1. Convergence of the subiterates. To simplify the presentation, we introduce the following notations related to the errors at each iteration

$$\begin{aligned} a_{(k)} &= z_{n+1/2}^+ - z_{(k)}^+, & b_{(k)} &= z_{n+1/2}^- - z_{(k)}^-, \\ \gamma_n &= \max\{\|\nabla z_{n+1/2}^+\|, \|\nabla z_{n+1/2}^-\|\}, & \delta &= \left(\frac{2(d-1)}{d^{3/2}}\right)^{d/4}. \end{aligned}$$

and a weighted $H^1(\Omega)$ norm of the errors $a_{(k)}, b_{(k)}$

$$\begin{aligned} \mathcal{G}_{(k)} &= \frac{4-d}{8} (\delta^2 \gamma_n)^{\frac{4}{4-d}} \left(\frac{d}{2} \frac{\nu + \nu_m}{\nu \nu_m}\right)^{\frac{d}{4-d}} (\|a_{(k)}\|^2 + \|b_{(k)}\|^2) \\ &\quad + \frac{\nu^2 - \nu \nu_m + \nu_m^2}{4(\nu + \nu_m)} (\|\nabla a_{(k)}\|^2 + \|\nabla b_{(k)}\|^2). \end{aligned}$$

The next result shows the $H^1(\Omega)$ strong convergence of the iterates $z_{(k)}^\pm$, under the following time step restriction

$$\tau_n \leq \frac{8}{4-d} \frac{1}{(\delta^2 \gamma_n)^{4/(4-d)}} \frac{\nu^2 - \nu \nu_m + \nu_m^2}{\nu^2 + \nu_m^2} \left(\frac{2\nu \nu_m}{d(\nu + \nu_m)}\right)^{d/(4-d)}. \quad (3.1)$$

THEOREM 3.1. *Assume that the time step τ_n satisfies condition (3.1). Then, the (1.6) sequence of iterates $\{z_{(k)}^\pm\}_{k \geq 0}$ converges linearly to $z_{n+1/2}^\pm$ in the $H^1(\Omega)$ norm*

$$\mathcal{G}_{(k)} \leq \left(1 - \frac{2\nu\nu_m}{\nu^2 + \nu\nu_m + \nu_m^2}\right) \mathcal{G}_{(k-1)}. \quad (3.2)$$

Proof. First, we subtract (1.6) from (1.5), and test the result with $a_{(k)}$ and $b_{(k)}$, respectively, to obtain

$$\begin{aligned} & \frac{2}{\tau_n} (\|a_{(k)}\|^2 + \|b_{(k)}\|^2) + \frac{\nu + \nu_m}{2} (\|\nabla a_{(k)}\|^2 + \|\nabla b_{(k)}\|^2) \\ & + \frac{\nu - \nu_m}{2} ((\nabla a_{(k)}, \nabla b_{(k-1)}) + (\nabla a_{(k-1)}, \nabla b_{(k)})) \\ & + \int_{\Omega} b_{(k-1)} \cdot \nabla z_{n+1/2}^+ a_{(k)} + \int_{\Omega} a_{(k)} \cdot \nabla z_{n+1/2}^- b_{(k)} = 0. \end{aligned}$$

Then, using the polarization identity on the mixed diffusion terms, we have

$$\begin{aligned} & \frac{\nu - \nu_m}{2} ((\nabla a_{(k)}, \nabla b_{(k-1)}) + (\nabla a_{(k-1)}, \nabla b_{(k)})) \\ & = -\frac{\nu + \nu_m}{4} (\|\nabla a_{(k)}\|^2 + \|\nabla b_{(k)}\|^2) - \frac{(\nu - \nu_m)^2}{4(\nu + \nu_m)} (\|\nabla a_{(k-1)}\|^2 + \|\nabla b_{(k-1)}\|^2) \\ & + \frac{|\nu - \nu_m|}{4} \left\| \sqrt{\frac{\nu + \nu_m}{|\nu - \nu_m|}} \nabla a_{(k)} + \text{sign}(\nu - \nu_m) \sqrt{\frac{|\nu - \nu_m|}{\nu + \nu_m}} \nabla b_{(k-1)} \right\|^2 \\ & + \frac{|\nu - \nu_m|}{4} \left\| \sqrt{\frac{\nu + \nu_m}{|\nu - \nu_m|}} \nabla b_{(k)} + \text{sign}(\nu - \nu_m) \sqrt{\frac{|\nu - \nu_m|}{\nu + \nu_m}} \nabla a_{(k-1)} \right\|^2, \end{aligned}$$

where

$$\text{sign}(x) := \begin{cases} -1, & \text{if } x < 0, \\ 0, & \text{if } x = 0, \\ 1, & \text{if } x > 0, \end{cases}$$

and therefore

$$\begin{aligned} & \frac{2}{\tau_n} (\|a_{(k)}\|^2 + \|b_{(k)}\|^2) + \frac{\nu + \nu_m}{4} (\|\nabla a_{(k)}\|^2 + \|\nabla b_{(k)}\|^2) \\ & + \frac{|\nu - \nu_m|}{4} \left\| \sqrt{\frac{\nu + \nu_m}{|\nu - \nu_m|}} \nabla a_{(k)} + \text{sign}(\nu - \nu_m) \sqrt{\frac{|\nu - \nu_m|}{\nu + \nu_m}} \nabla b_{(k-1)} \right\|^2 \\ & + \frac{|\nu - \nu_m|}{4} \left\| \sqrt{\frac{\nu + \nu_m}{|\nu - \nu_m|}} \nabla b_{(k)} + \text{sign}(\nu - \nu_m) \sqrt{\frac{|\nu - \nu_m|}{\nu + \nu_m}} \nabla a_{(k-1)} \right\|^2 \\ & + \int_{\Omega} b_{(k-1)} \cdot \nabla z_{n+1/2}^+ a_{(k)} + \int_{\Omega} a_{(k)} \cdot \nabla z_{n+1/2}^- b_{(k)} \\ & = \frac{(\nu - \nu_m)^2}{4(\nu + \nu_m)} (\|\nabla a_{(k-1)}\|^2 + \|\nabla b_{(k-1)}\|^2). \end{aligned}$$

Now we apply the Ladyzhenskaya inequality (2.10) to the convective terms to obtain

$$\int_{\Omega} b_{(k-1)} \cdot \nabla z_{n+1/2}^+ a_{(k)} + \int_{\Omega} a_{(k-1)} \cdot \nabla z_{n+1/2}^- b_{(k)}$$

$$\begin{aligned}
&\geq -\frac{4-d}{8} \left(\frac{2(d-1)}{d^{3/2}} \right)^{\frac{2d}{4-d}} \left(\frac{d}{2} \right)^{d/(4-d)} \left(\frac{\nu + \nu_m}{\nu \nu_m} \right)^{\frac{d}{4-d}} \gamma_n^{\frac{4}{4-d}} \left(\|a_{(k)}\|^2 + \|b_{(k)}\|^2 \right) \\
&\quad - \frac{4-d}{8} \left(\frac{2(d-1)}{d^{3/2}} \right)^{\frac{2d}{4-d}} \left(\frac{d}{2} \right)^{d/(4-d)} \left(\frac{\nu + \nu_m}{\nu \nu_m} \right)^{\frac{d}{4-d}} \gamma_n^{\frac{4}{4-d}} \left(\|a_{(k-1)}\|^2 + \|b_{(k-1)}\|^2 \right) \\
&\quad - \frac{1}{4} \frac{\nu \nu_m}{\nu + \nu_m} \left(\|\nabla a_{(k)}\|^2 + \|\nabla b_{(k)}\|^2 \right) - \frac{1}{4} \frac{\nu \nu_m}{\nu + \nu_m} \left(\|\nabla a_{(k-1)}\|^2 + \|\nabla b_{(k-1)}\|^2 \right).
\end{aligned}$$

Finally, using this inequality in the relation above implies

$$\begin{aligned}
&\left(\frac{2}{\tau_n} - \frac{4-d}{8} (\delta^2 \gamma_n)^{\frac{4}{4-d}} \left(\frac{d}{2} \frac{\nu + \nu_m}{\nu \nu_m} \right)^{\frac{d}{4-d}} \right) (\|a_{(k)}\|^2 + \|b_{(k)}\|^2) \\
&\quad + \frac{\nu^2 + \nu \nu_m + \nu_m^2}{4(\nu + \nu_m)} (\|\nabla a_{(k)}\|^2 + \|\nabla b_{(k)}\|^2) \\
&\leq \frac{4-d}{8} (\delta^2 \gamma_n)^{\frac{4}{4-d}} \left(\frac{d}{2} \frac{\nu + \nu_m}{\nu \nu_m} \right)^{\frac{d}{4-d}} (\|a_{(k-1)}\|^2 + \|b_{(k-1)}\|^2) \\
&\quad + \frac{\nu^2 - \nu \nu_m + \nu_m^2}{4(\nu + \nu_m)} (\|\nabla a_{(k-1)}\|^2 + \|\nabla b_{(k-1)}\|^2).
\end{aligned}$$

Hence, under the time step restriction (3.1), the above estimate yields the linear convergence relation (3.2). \square

3.2. Stability and a balance of energy. Now we consider the stability of the algorithm (1.4). We denote the discrete kinetic energy of the system by \mathcal{E}^N , the viscous dissipation rate by \mathcal{D}^N :

$$\begin{aligned}
\mathcal{E}^N &= \frac{1}{2} (\|z_N^+\|^2 + \|z_N^-\|^2), \\
\mathcal{D}^N &= \min\{\nu, \nu_m\} \sum_{n=1}^{N-1} \tau_n (\|\nabla z_{n+1/2}^+\|^2 + \|\nabla z_{n+1/2}^-\|^2) \\
&\quad + |v^-| \sum_{n=1}^{N-1} \tau_n \|\nabla z_{n+1/2}^+ + \text{sign}(v^-) \nabla z_{n+1/2}^-\|^2.
\end{aligned} \tag{3.3}$$

THEOREM 3.2. *The algorithm in (1.4) is unconditionally stable and satisfies*

$$\begin{aligned}
&\mathcal{E}^N + \frac{1}{2} \mathcal{D}^N + \frac{|v^-|}{2} \sum_{n=1}^{N-1} \tau_n \|\nabla z_{n+1/2}^+ + \text{sign}(v^-) \nabla z_{n+1/2}^-\|^2 \\
&\leq \sum_{n=1}^{N-1} \frac{\tau_n}{\min\{\nu, \nu_m\}} \|f(t_{n+1/2})\|_{-1}^2 + \mathcal{E}^0.
\end{aligned} \tag{3.4}$$

Moreover, in the absence of external force f , the following energy balance holds

$$\mathcal{E}^N + \mathcal{D}^N = \mathcal{E}^0. \tag{3.5}$$

Proof. We first take inner product of (1.4) with $2z_{n+1/2}^\pm$, and use the skew-symmetry properties (2.7), (2.8) to obtain

$$\frac{1}{\tau_n} (\|z_{n+1}^\pm\|^2 - \|z_n^\pm\|^2) + 2\nu^+ \|\nabla z_{n+1/2}^\pm\|^2 + 2\nu^- (z_{n+1/2}^\mp, z_{n+1/2}^\pm)$$

$$= 2(f(t_{n+1/2}), z_{n+1/2}^{\pm}). \quad (3.6)$$

Then we use the following polarization identity

$$\begin{aligned} & \nu^- (\nabla z_{n+1/2}^{\mp}, \nabla z_{n+1/2}^{\pm}) \\ &= \frac{|\nu^-|}{2} \|\nabla z_{n+1/2}^{\mp} + \text{sign}(\nu^-) \nabla z_{n+1/2}^{\pm}\|^2 - \frac{|\nu^-|}{2} (\|\nabla z_{n+1/2}^{\mp}\|^2 + \|\nabla z_{n+1/2}^{\pm}\|^2), \end{aligned}$$

to obtain

$$\begin{aligned} & \frac{1}{2\tau_n} (\|z_{n+1}^+\|^2 + \|z_{n+1}^-\|^2 - \|z_n^+\|^2 - \|z_n^-\|^2) \\ &+ (\nu^+ - |\nu^-|) (\|\nabla z_{n+1/2}^+\|^2 + \|\nabla z_{n+1/2}^-\|^2) + |\nu^-| \|\nabla z_{n+1/2}^+ + \text{sign}(\nu^-) \nabla z_{n+1/2}^-\|^2 \\ &= (f(t_{n+1/2}), z_{n+1/2}^+) + (f(t_{n+1/2}), z_{n+1/2}^-). \end{aligned} \quad (3.7)$$

Using $\nu^+ - |\nu^-| = \min\{\nu, \nu_m\}$, the definition of dual norm (2.1), and Young's inequality we have

$$\begin{aligned} & \frac{1}{2\tau_n} (\|z_{n+1}^+\|^2 + \|z_{n+1}^-\|^2 - \|z_n^+\|^2 - \|z_n^-\|^2) \\ &+ \frac{1}{2} \min\{\nu, \nu_m\} (\|\nabla z_{n+1/2}^+\|^2 + \|\nabla z_{n+1/2}^-\|^2) + |\nu^-| \|\nabla z_{n+1/2}^+ + \text{sign}(\nu^-) \nabla z_{n+1/2}^-\|^2 \\ &\leq \frac{1}{\min\{\nu, \nu_m\}} \|f(t_{n+1/2})\|_{-1}^2. \end{aligned} \quad (3.8)$$

Finally, if we multiply (3.8) by τ_n and sum over n from 1 to $N-1$, we obtain (3.4). In the case when the source function f vanishes, summation of (3.7) over n from 1 to $N-1$ yields (3.5). \square

3.3. Conservation of quadratic invariants: energy, cross-helicity and magnetic-helicity. We note that the fully coupled system (1.4) can be equivalently written as

$$\left\{ \begin{aligned} & \frac{u_{n+1} - u_n}{\tau_n} - (B_{n+1/2} \cdot \nabla) B_{n+1/2} + (u_{n+1/2} \cdot \nabla) u_{n+1/2} - \nu \Delta u_{n+1/2} \\ & \quad + \nabla \left(\frac{p_{n+1/2}^+ + p_{n+1/2}^-}{2} \right) = f(t_{n+1/2}), \\ & \frac{B_{n+1} - B_n}{\tau_n} + (u_{n+1/2} \cdot \nabla) B_{n+1/2} - (B_{n+1/2} \cdot \nabla) u_{n+1/2} - \nu_m \Delta B_{n+1/2} \\ & \quad + \nabla \left(\frac{p_{n+1/2}^+ - p_{n+1/2}^-}{2} \right) = 0, \\ & \nabla \cdot u_{n+1/2} = 0, \quad \nabla \cdot B_{n+1/2} = 0, \end{aligned} \right. \quad (3.9)$$

where by Step 2 in (1.5) we have $u_{n+1/2} = (u_{n+1} + u_n)/2$ and $B_{n+1/2} = (B_{n+1} + B_n)/2$.

We denote the energy, the cross-helicity and the magnetic-helicity corresponding to the solution at time t_n of algorithm (3.9) by

$$\mathcal{E}_n = \frac{1}{2} \int_{\Omega} (|u_n|^2 + |B_n|^2) dx, \quad \mathcal{H}_{C_n} = \frac{1}{2} \int_{\Omega} u_n \cdot B_n dx, \quad \mathcal{H}_{M_n} = \frac{1}{2} \int_{\Omega} \mathbb{A}_n \cdot B_n dx.$$

THEOREM 3.3. *The algorithm in (1.4) or (3.9), conserves the energy, cross-helicity and magnetic-helicity*

$$\mathcal{E}_n = \mathcal{E}_0, \quad \mathcal{H}_{C_n} = \mathcal{H}_{C_0}, \quad \mathcal{H}_{M_n} = \mathcal{H}_{M_0},$$

in the ideal case, i.e., in the absence of external forcing terms, and for zero kinematic viscosity and magnetic diffusivity.

Proof. We assume that $f = 0$, and $\nu = \nu_m = 0$. First, we take inner product of first equation of (3.9) with $u_{n+1/2}$, the second equation of (3.9) with $B_{n+1/2}$ and use the skew-symmetry properties (2.7), (2.8) to obtain

$$\frac{1}{2}(\|u_{n+1}\|^2 + \|B_{n+1}\|^2) - \frac{1}{2}(\|u_n\|^2 + \|B_n\|^2) = 0. \quad (3.10)$$

Summation of (3.10) over n from 1 to $N-1$ and proves the conservation of the model energy, i.e., $\mathcal{E}_N = \mathcal{E}_0$.

Secondly, we take the inner product of the first equation in (3.9) with $B_{n+1/2}$, the second equation of (3.9) with $u_{n+1/2}$, to obtain

$$\begin{aligned} \frac{1}{2\tau_n}(u_{n+1} - u_n, B_{n+1} + B_n) + ((u_{n+1/2} \cdot \nabla)u_{n+1/2}, B_{n+1/2}) &= 0, \\ \frac{1}{2\tau_n}(B_{n+1} - B_n, u_{n+1} + u_n) + ((u_{n+1/2} \cdot \nabla)B_{n+1/2}, u_{n+1/2}) &= 0, \end{aligned}$$

and using (2.7), (2.8), these yield

$$\frac{1}{\tau_n} \int_{\Omega} u_{n+1} \cdot B_{n+1} dx - \frac{1}{\tau_n} \int_{\Omega} u_n \cdot B_n dx = 0, \quad (3.11)$$

which proves the conservation of cross helicity, i.e., $\mathcal{H}_{C_N} = \mathcal{H}_{C_0}$.

For the result on the magnetic helicity, we begin by recalling (see e.g., [20, Theorem 3.2, Chapter I]) that, since $\nabla \cdot B_n = 0$, there exists a function $\mathbb{A}_n \in (H^1(\Omega))^d$ such that $B_n = \nabla \times \mathbb{A}_n$ for all n . Moreover, $\nabla \cdot \mathbb{A}_n = 0$ and $\mathbb{A}_n = 0$ on the boundary. Next, we take the inner product of the second equation in (3.9) with $\mathbb{A}_{n+1/2} = (\mathbb{A}_{n+1} + \mathbb{A}_n)/2$

$$\begin{aligned} \frac{1}{\tau_n}(B_{n+1} - B_n, \mathbb{A}_{n+1/2}) \\ + ((u_{n+1/2} \cdot \nabla)B_{n+1/2}, \mathbb{A}_{n+1/2}) - ((B_{n+1/2} \cdot \nabla)u_{n+1/2}, \mathbb{A}_{n+1/2}) &= 0. \end{aligned} \quad (3.12)$$

Then, we use the identity

$$\nabla \times (B \times u) = (\nabla \cdot u)B + (u \cdot \nabla)B - (\nabla \cdot B)u - (B \cdot \nabla)u,$$

to write the convective terms as follows

$$\begin{aligned} &((u_{n+1/2} \cdot \nabla)B_{n+1/2}, \mathbb{A}_{n+1/2}) - ((B_{n+1/2} \cdot \nabla)u_{n+1/2}, \mathbb{A}_{n+1/2}) \\ &= (\nabla \times (B_{n+1/2} \times u_{n+1/2}), \mathbb{A}_{n+1/2}) - ((\nabla \cdot u_{n+1/2})B_{n+1/2}, \mathbb{A}_{n+1/2}) \\ &\quad + ((\nabla \cdot B_{n+1/2})u_{n+1/2}, \mathbb{A}_{n+1/2}) \\ &= (\nabla \times ((\nabla \times \mathbb{A}_{n+1/2}) \times u_{n+1/2}), \mathbb{A}_{n+1/2}) \\ &= ((\nabla \times \mathbb{A}_{n+1/2}) \times u_{n+1/2}, \nabla \times \mathbb{A}_{n+1/2}) - \int_{\partial\Omega} ((\nabla \times \mathbb{A}_{n+1/2}) \times u_{n+1/2}) \times \mathbb{A}_{n+1/2} = 0, \end{aligned} \quad (3.13)$$

where the last equality comes from the homogeneous Dirichlet boundary condition on the velocity $u|_{\partial\Omega}=0$, and the orthogonality of $\nabla \times \mathbb{A}_{n+1/2}$ and $(\nabla \times \mathbb{A}_{n+1/2}) \times u_{n+1/2}$. Using (3.13) in (3.12) gives

$$\int_{\Omega} \mathbb{A}_{n+1} \cdot B_{n+1} dx + \int_{\Omega} \mathbb{A}_n \cdot B_{n+1} dx - \int_{\Omega} \mathbb{A}_{n+1} \cdot B_n dx = \int_{\Omega} \mathbb{A}_n \cdot B_n dx. \quad (3.14)$$

Finally, by the Gauss' divergence theorem we have

$$\int_{\Omega} \mathbb{A}_n \cdot B_{n+1} dx - \int_{\Omega} \mathbb{A}_{n+1} \cdot B_n dx = \int_{\Omega} \nabla \cdot (\mathbb{A}_{n+1} \times \mathbb{A}_n) dx = 0,$$

and therefore (3.14) implies the conservation of magnetic-helicity $\mathcal{H}_{M_N} = \mathcal{H}_{M_0}$. \square

3.4. Error Analysis. In this section, $z^{\pm}(t_n)$ represent the true solutions of (1.3) at time t_n . For the fully space-time discretization, $z_n^{\pm,h} \in X^h$ and $p_{n+1/2}^{\pm,h} \in Q^h$ are numerical approximations of $z^{\pm}(t_n)$ and $p(t_{n+1/2})$ respectively.

The variational formulation of the fully-decoupled algorithm in (1.4) is: given $z_n^{\pm,h} \in X^h$, we solve $z_{n+1}^{\pm,h} \in X^h, p_{n+1/2}^{\pm,h} \in Q^h$ such that for all $(v^h, q^h) \in X^h \times Q^h$,

$$\begin{cases} \left(\frac{z_{n+1}^{\pm,h} - z_n^{\pm,h}}{\tau_n}, v^h \right) \mp \mathcal{N}(B_o, z_{n+1/2}^{\pm,h}, v^h) + \mathcal{N}(z_{n+1/2}^{\mp,h}, z_{n+1/2}^{\pm,h}, v^h) \\ + \nu^+ (\nabla z_{n+1/2}^{\pm,h}, \nabla v^h) + \nu^- (\nabla z_{n+1/2}^{\mp,h}, \nabla v^h) - (p_{n+1/2}^{\pm,h}, \nabla \cdot v^h) = (f(t_{n+1/2}), v^h), \\ (\nabla \cdot z_{n+1/2}^{\pm,h}, q^h) = 0. \end{cases} \quad (3.15)$$

The following result recalls the consistency of the midpoint finite difference method.

LEMMA 3.4. *For any given nodes $\{t_n\}_{n=0}^N$ on the time interval $[0, T]$, if the mapping $u : [0, T] \rightarrow H^\ell(\Omega)$ is smooth enough, then*

$$\left\| (u(\cdot, t_{n+1}) + u(\cdot, t_n))/2 - u(\cdot, t_{n+1/2}) \right\|_{\ell} \leq C \tau_n^3 \int_{t_n}^{t_{n+1}} \|u_{tt}(\cdot, t)\|_{\ell}^2 dt, \quad (3.16)$$

$$\left\| \frac{u(\cdot, t_{n+1}) - u(\cdot, t_n)}{\tau_n} - u(\cdot, t_{n+1/2}) \right\|_{\ell} \leq C \tau_n^3 \int_{t_n}^{t_{n+1}} \|u_{ttt}(\cdot, t)\|_{\ell}^2 dt. \quad (3.17)$$

Proof. A direct calculation involving the Taylor expansion with integral remainder about $t_{n+1/2}$. \square

We also need the following Bochner spaces on the time interval $[0, T]$

$$L^p(0, T; (H^\ell(\Omega))^d) = \left\{ v(\cdot, t) \in (H^\ell(\Omega))^d : \|v\|_{p, \ell} = \left(\int_0^T \|v(\cdot, t)\|_{\ell}^p dt \right)^{1/p} < \infty \right\},$$

$$L^\infty(0, T; (H^\ell(\Omega))^d) = \left\{ v(\cdot, t) \in (H^\ell(\Omega))^d : \|v\|_{\infty, \ell} = \sup_{0 < t < T} \|v(\cdot, t)\|_{\ell} < \infty \right\},$$

$$L^p(0, T; X') = \left\{ v(\cdot, t) \in X' : \|v\|_{p, -1} = \left(\int_0^T \|v(\cdot, t)\|_{-1}^p dt \right)^{1/p} < \infty \right\},$$

and the corresponding discrete Bochner spaces

$$\begin{aligned} & \ell^\infty(\{t_n\}_{n=0}^N; (H^\ell(\Omega))^d) \\ & := \left\{ v(\cdot, t_n) \in (H^\ell(\Omega))^d : \|v\|_{\infty, \ell} := \max_{0 \leq n \leq N} \|v(\cdot, t_n)\|_{\ell} < \infty \right\}, \end{aligned}$$

$$\begin{aligned}
& \ell^{\infty,1/2}(\{t_n\}_{n=0}^N; (H^\ell(\Omega))^d) \\
& := \left\{ v(\cdot, t_{n+1/2}) \in (H^\ell(\Omega))^d : \|v\|_{\infty, \ell, 1/2} := \max_{1 \leq n \leq N-1} \|v(\cdot, t_{n+1/2})\|_\ell < \infty \right\}, \\
& \ell^{p,1/2}(\{t_n\}_{n=0}^N; (H^\ell(\Omega))^d) \\
& := \left\{ v(\cdot, t_{n+1/2}) \in (H^\ell(\Omega))^d : \|v\|_{p, \ell, 1/2} := \left(\sum_{n=1}^{N-1} \tau_n \|v(\cdot, t_{n+1/2})\|_\ell^p \right)^{1/p} < \infty \right\}, \\
& \ell^{p,1/2}(\{t_n\}_{n=0}^N; X') \\
& := \left\{ v(\cdot, t_{n+1/2}) \in X' : \|v\|_{p, \ell, -1} := \left(\sum_{n=1}^{N-1} \tau_n \|v(\cdot, t_{n+1/2})\|_{-1}^p \right)^{1/p} < \infty \right\}.
\end{aligned}$$

We denote the errors in the algorithm (3.15) at time t_n by $e_n^\pm = z_n^{\pm, h} - z^\pm(t_n)$.

THEOREM 3.5. *We assume that (z^\pm, p) in (1.3) satisfies the regularity assumptions*

$$\begin{aligned}
z^\pm & \in \ell^\infty(\{t_n\}_{n=0}^N; (H^\ell)^d) \cap \ell^{\infty,1/2}(\{t_n\}_{n=0}^N; (H^\ell)^d) \cap \ell^{2,1/2}(\{t_n\}_{n=0}^N; (H^{r+1})^d \cap (H^2)^d), \\
z^\pm & \in \ell^{4,1/2}(\{t_n\}_{n=0}^N; (H^1)^d) \cap L^4(0, T; (H^1)^d) \\
z_t^\pm & \in L^2(0, T; (H^{r+1})^d), \quad z_{tt}^\pm \in L^2(0, T; (H^{r+1})^d \cap (H^1)^d), \\
z_{ttt}^\pm & \in L^2(0, T; X'), \quad p \in \ell^{2,1/2}(\{t_n\}_{n=0}^N; H^{s+1}).
\end{aligned} \tag{3.18}$$

and time step size τ_n satisfies

$$\tau_n < \frac{1}{16(C_1^* h Z_n^{(1)} + 256 C_2^* Z_n^{(2)})}, \quad \forall n = 1, 2, \dots, N-1, \tag{3.19}$$

where

$$\begin{aligned}
C_1^* &= \frac{2(3(d-1))^{2d/3} C_P^{3-d} C_I (C_A^{1,0})^2}{\epsilon \nu^* d^{7d/6}} \left(1 + \frac{1}{\beta_{\text{is}}}\right)^2, \quad C_2^* = \frac{(3(d-1))^{4d/3} C_P^{2(3-d)}}{32(\nu^*)^3 d^{7d/3}}, \\
Z_n^{(1)} &= \frac{1}{2} \max \{ |z^+(t_{n+1}) + z^+(t_n)|_2, |z^-(t_{n+1}) + z^-(t_n)|_2 \}, \\
Z_n^{(2)} &= \frac{1}{2} \max \{ \|\nabla(z^+(t_{n+1}) + z^+(t_n))\|^4, \|\nabla(z^-(t_{n+1}) + z^-(t_n))\|^4 \},
\end{aligned}$$

$\nu^* = \nu^+ - |\nu^-| = \min\{\nu, \nu_m\}$, and C_P represents the constant in the Poincaré inequality. Then the following error estimates hold

$$\begin{aligned}
\|e_N^+\|^2 + \|e_N^-\|^2 & \leq C h^{2r} (\|z^+\|_{\infty, r+1}^2 + \|z^-\|_{\infty, r+1}^2) \\
& + \exp \left(C \sum_{n=1}^{N-1} (C_1^* h Z_n^{(1)} + C_2^* Z_n^{(2)}) \tau_n \right) F(h^{2r}, h^{2s+2}, \tau_{\max}^4, \|B_o\|^2),
\end{aligned} \tag{3.20}$$

and

$$\begin{aligned}
& \nu^* \sum_{n=0}^{N-1} \tau_n (\|\nabla(e_{n+1}^+ + e_n^+)/2\|^2 + \|\nabla(e_{n+1}^- + e_n^-)/2\|^2) \\
& \leq C \nu^* h^{2r} (\tau_{\max}^4 \|z^\pm\|_{2, r+1}^2 + \|z^\pm\|_{2, r+1, 1/2}^2)
\end{aligned}$$

$$+ \exp\left(C \sum_{n=1}^{N-1} (C_1^* h Z_n^{(1)} + C_2^* Z_n^{(2)}) \tau_n\right) F(h^{2r}, h^{2s+2}, \tau_{\max}^4, \|B_o\|^2),$$

where $\tau_{\max} = \max_{0 \leq n \leq N} \{\tau_n\}$ and

$$\begin{aligned} & F(h^{2r}, h^{2s+2}, \tau_{\max}^4, \|B_o\|^2) \\ &= \frac{h^{2r+2}}{\nu^*} (\|z^+\|_{2,r+1}^2 + \|z^-\|_{2,r+1}^2) + \frac{((\nu^+)^2 + (\nu^-)^2) h^{2r} \tau_{\max}^4}{\nu^*} (\|z_{tt}^+\|_{2,r+1}^2 + \|z_{tt}^-\|_{2,r+1}^2) \\ &+ \frac{((\nu^+)^2 + (\nu^-)^2) h^{2r}}{\nu^*} (\|z^+\|_{2,r+1,1/2}^2 + \|z^-\|_{2,r+1,1/2}^2) \\ &+ \frac{(\nu^-)^2 \tau_{\max}^4}{\nu^*} (\|\nabla z_{tt}^+\|_{2,0}^2 + \|\nabla z_{tt}^-\|_{2,0}^2) + \frac{h^{2s+2}}{\nu^*} (\|p^+\|_{2,s+1,1/2}^2 + \|p^-\|_{2,s+1,1/2}^2) \\ &+ \frac{\tau_{\max}^4}{\nu^*} (\|\nabla z_{ttt}^+\|_{2,0}^2 + \|\nabla z_{ttt}^-\|_{2,0}^2) + \frac{\tau_{\max}^4}{\nu^*} \|B_o\|^2 (\|\nabla z_{tt}^+\|_{2,0}^2 + \|\nabla z_{tt}^-\|_{2,0}^2) \\ &+ \frac{h^{2r} \tau_{\max}^4}{\nu^*} \|B_o\|^2 (\|z_{tt}^\pm\|_{2,r+1}^2 + \|z_{tt}^\pm\|_{2,r+1}^2) \\ &+ \frac{h^{2r}}{\nu^*} \|B_o\|^2 (\|z^+\|_{2,r+1,1/2}^2 + \|z^-\|_{2,r+1,1/2}^2) \\ &+ \frac{\tau_{\max}^4}{\nu^*} (\|z^-\|_{\infty,1}^2 \|\nabla z_{tt}^+\|_{2,0}^2 + \|z^+\|_{\infty,1}^2 \|\nabla z_{tt}^-\|_{2,0}^2 + \|z^+\|_{\infty,1,1/2}^2 \|\nabla z_{tt}^-\|_{2,0}^2 \\ &\quad + \|z^-\|_{\infty,1,1/2}^2 \|\nabla z_{tt}^+\|_{2,0}^2) \\ &+ \frac{h^{2r} \tau_{\max}^4}{\nu^*} (\|\nabla z^-\|_{\infty,0}^2 \|z_{tt}^+\|_{2,r+1}^2 + \|\nabla z^+\|_{\infty,0}^2 \|z_{tt}^-\|_{2,r+1}^2) \\ &+ \frac{h^{2r}}{\nu^*} (\|z^+\|_{2,r+1,1/2}^2 + \|z^-\|_{2,r+1,1/2}^2) + (\|\xi_0^{+,h}\|^2 + \|\xi_0^{-,h}\|^2). \end{aligned}$$

Proof. The true solutions of (1.3) at time $t_{n+1/2}$ satisfies

$$\begin{aligned} & \left(\frac{z^\pm(t_{n+1}) - z^\pm(t_n)}{\tau_n}, v^h \right) \mp \mathcal{N}(B_o, z^\pm(t_{n+1/2}), v^h) + \mathcal{N}(z^\mp(t_{n+1/2}), z^\pm(t_{n+1/2}), v^h) \\ &+ \nu^+ (\nabla z^\pm(t_{n+1/2}), \nabla v^h) + \nu^- (\nabla z^\mp(t_{n+1/2}), \nabla v^h) - (p^\pm(t_{n+1/2}), \nabla \cdot v^h) \\ &= (f(t_{n+1/2}), v^h) + \left(\frac{z^\pm(t_{n+1}) - z^\pm(t_n)}{\tau_n} - z_t^\pm(t_{n+1/2}), v^h \right), \quad \forall v^h \in V^h. \end{aligned} \tag{3.21}$$

We denote by $I_{\text{St}} z_n^\pm$ the velocity components of Stokes projection of $(z_n^\pm, 0)$ onto $V^h \times Q^h$ and decompose the error e_n^\pm as

$$e_n^\pm = \xi_n^{\pm,h} + \eta^\pm(t_n), \quad \xi_n^{\pm,h} := z_n^{\pm,h} - I_{\text{St}} z^\pm(t_n), \quad \eta^\pm(t_n) := I_{\text{St}} z^\pm(t_n) - z^\pm(t_n). \tag{3.22}$$

For convenience of the presentation, we denote

$$\begin{aligned} \xi_{n+1/2}^\pm &:= (\xi_{n+1}^\pm + \xi_n^\pm)/2, \\ z_{n+1/2}^\pm &:= (z^\pm(t_{n+1}) + z^\pm(t_n))/2, \quad \eta_{n+1/2}^\pm := (\eta^\pm(t_{n+1}) + \eta^\pm(t_n))/2. \end{aligned}$$

We subtract (3.21) from the first equation of (3.15) to obtain:

$$\left(\frac{e_{n+1}^\pm - e_n^\pm}{\tau_n}, v^h \right) + \nu^+ (\nabla(e_{n+1}^\pm + e_n^\pm)/2, \nabla v^h) + \nu^- (\nabla(e_{n+1}^\mp + e_n^\mp)/2, \nabla v^h)$$

$$\begin{aligned}
& \mp \mathcal{N}(B_\circ, (e_{n+1}^\mp + e_n^\mp)/2, v^h) \\
&= \nu^+ (\nabla z^\pm(t_{n+1/2}) - \nabla((z^\pm(t_{n+1}) + z^\pm(t_n))/2), \nabla v^h) \\
& \quad + \nu^- (\nabla z^\mp(t_{n+1/2}) - \nabla((z^\mp(t_{n+1}) + z^\mp(t_n))/2), \nabla v^h) \\
& \quad \pm \mathcal{N}(B_\circ, (z^\pm(t_{n+1}) + z^\pm(t_n))/2 - z^\pm(t_{n+1/2}), v^h) - (p^\pm(t_{n+1/2}) - q^h, \nabla \cdot v^h) \\
& \quad + \mathcal{N}(z^\mp(t_{n+1/2}), z^\pm(t_{n+1/2}), v^h) - \mathcal{N}(z_{n+1/2}^{\mp,h}, z_{n+1/2}^{\pm,h}, v^h) \\
& \quad - \left(\frac{z^\pm(t_{n+1}) - z^\pm(t_n)}{\tau_n} - z_t^\pm(t_{n+1/2}), v^h \right), \quad \forall (v^h, q^h) \in V^h \times Q^h.
\end{aligned}$$

By the decomposition of the error e_n^\pm (3.22), the above can be equivalently written as

$$\begin{aligned}
& \left(\frac{\xi_{n+1}^{\pm,h} - \xi_n^{\pm,h}}{\tau_n}, v^h \right) + \nu^+ (\nabla \xi_{n+1/2}^{\pm,h}, \nabla v^h) + \nu^- (\nabla \xi_{n+1/2}^{\mp,h}, \nabla v^h) \mp \mathcal{N}(B_\circ, \xi_{n+1/2}^{\pm,h}, v^h) \\
&= - \left(\frac{\eta^\pm(t_{n+1}) - \eta^\pm(t_n)}{\tau_n}, v^h \right) - \nu^+ (\nabla \eta_{n+1/2}^\pm, \nabla v^h) - \nu^- (\nabla \eta_{n+1/2}^\mp, \nabla v^h) \pm \mathcal{N}(B_\circ, \eta_{n+1/2}^\pm, v^h) \\
& \quad + \nu^+ (\nabla z^\pm(t_{n+1/2}) - \nabla z_{n+1/2}^\pm, \nabla v^h) + \nu^- (\nabla z^\mp(t_{n+1/2}) - \nabla z_{n+1/2}^\mp, \nabla v^h) \\
& \quad - (p^\pm(t_{n+1/2}) - q^h, \nabla \cdot v^h) - \left(\frac{z^\pm(t_{n+1}) - z^\pm(t_n)}{\tau_n} - z_t^\pm(t_{n+1/2}), v^h \right) \\
& \quad \pm \mathcal{N}(B_\circ, z_{n+1/2}^\pm - z^\pm(t_{n+1/2}), v^h) + \mathcal{N}(z^\mp(t_{n+1/2}), z^\pm(t_{n+1/2}), v^h) \\
& \quad - \mathcal{N}(z_{n+1/2}^{\mp,h}, z_{n+1/2}^{\pm,h}, v^h).
\end{aligned}$$

We set $v^h = \xi_{n+1/2}^{\pm,h}$ and use skew-symmetry of \mathcal{N} to obtain

$$\begin{aligned}
& \frac{1}{2\tau_n} (\|\xi_{n+1}^{\pm,h}\|^2 - \|\xi_n^{\pm,h}\|^2) + \nu^+ \|\nabla \xi_{n+1/2}^{\pm,h}\|^2 + \nu^- (\nabla \xi_{n+1/2}^{\mp,h}, \nabla \xi_{n+1/2}^{\pm,h}) \quad (3.23) \\
&= - \left(\frac{\eta^\pm(t_{n+1}) - \eta^\pm(t_n)}{\tau_n}, \xi_{n+1/2}^{\pm,h} \right) - \nu^+ (\nabla \eta_{n+1/2}^\pm, \nabla \xi_{n+1/2}^{\pm,h}) - \nu^- (\nabla \eta_{n+1/2}^\mp, \nabla \xi_{n+1/2}^{\pm,h}) \\
& \quad + \nu^+ (\nabla z^\pm(t_{n+1/2}) - \nabla z_{n+1/2}^\pm, \nabla \xi_{n+1/2}^{\pm,h}) + \nu^- (\nabla z^\mp(t_{n+1/2}) - \nabla z_{n+1/2}^\mp, \nabla \xi_{n+1/2}^{\pm,h}) \\
& \quad - (p^\pm(t_{n+1/2}) - q^h, \nabla \cdot \xi_{n+1/2}^{\pm,h}) - \left(\frac{z^\pm(t_{n+1}) - z^\pm(t_n)}{\tau_n} - z_t^\pm(t_{n+1/2}), \xi_{n+1/2}^{\pm,h} \right) \\
& \quad \pm \mathcal{N}(B_\circ, \eta_{n+1/2}^\pm, \xi_{n+1/2}^{\pm,h}) \pm \mathcal{N}(B_\circ, z_{n+1/2}^\pm - z^\pm(t_{n+1/2}), \xi_{n+1/2}^{\pm,h}) \\
& \quad + \mathcal{N}(z^\mp(t_{n+1/2}), z^\pm(t_{n+1/2}), \xi_{n+1/2}^{\pm,h}) - \mathcal{N}(z_{n+1/2}^\mp, z_{n+1/2}^\pm, \xi_{n+1/2}^{\pm,h}) \\
& \quad + \mathcal{N}(z_{n+1/2}^\mp, z_{n+1/2}^\pm, \xi_{n+1/2}^{\pm,h}) - \mathcal{N}(z_{n+1/2}^{\mp,h}, z_{n+1/2}^{\pm,h}, \xi_{n+1/2}^{\pm,h}) = I_1 + \dots + I_{11}.
\end{aligned}$$

Now we address each of the terms on the right hand side of (3.23). By the Cauchy-Schwarz, Poincaré and Young's inequalities, the estimate of the Stokes projection (2.6), the approximations in (2.2) and Hölder's inequality we have

$$\begin{aligned}
I_1 &= - \left(\frac{\eta^\pm(t_{n+1}) - \eta^\pm(t_n)}{\tau_n}, \xi_{n+1/2}^{\pm,h} \right) \quad (3.24) \\
&\leq \frac{C(\epsilon)}{\tau_n^2 \nu^*} \|\eta^\pm(t_{n+1}) - \eta^\pm(t_n)\|^2 + \epsilon \nu^* \|\nabla \xi_{n+1/2}^{\pm,h}\|^2 \\
&\leq \frac{C(\epsilon) h^{2r+2}}{\tau_n^2 \nu^*} \|z^\pm(t_{n+1}) - z^\pm(t_n)\|_{r+1}^2 + \epsilon \nu^* \|\nabla \xi_{n+1/2}^{\pm,h}\|^2,
\end{aligned}$$

$$\leq \frac{C(\epsilon)h^{2r+2}}{\tau_n\nu^*} \int_{t_n}^{t_{n+1}} \|z^\pm\|_{r+1}^2 dt + \epsilon\nu^* \|\nabla \xi_{n+1/2}^{\pm,h}\|^2,$$

where $\epsilon > 0$ is a constant to be chosen later, and $C(\epsilon) > 0$ is a constant depending on ϵ . Using the Cauchy-Schwarz, Young's inequality, the estimate (2.6), the approximations (2.2) and (3.16) we also get

$$\begin{aligned} I_2 &= -\nu^+ (\nabla \eta_{n+1/2}^\pm, \nabla \xi_{n+1/2}^{\pm,h}) \leq C\nu^+ h^r \|z_{n+1/2}^\pm\|_{r+1} \|\nabla \xi_{n+1/2}^{\pm,h}\| \\ &\leq \frac{C(\epsilon)(\nu^+)^2 h^{2r}}{\nu^*} (\|z_{n+1/2}^\pm - z(t_{n+1/2})\|_{r+1}^2 + \|z(t_{n+1/2})\|_{r+1}^2) + \epsilon\nu^* \|\nabla \xi_{n+1/2}^{\pm,h}\|^2 \\ &\leq \frac{C(\epsilon)(\nu^+)^2 h^{2r}}{\nu^*} \left(\tau_{\max}^3 \int_{t_n}^{t_{n+1}} \|z_{tt}^\pm\|_{r+1}^2 dt + \|z^\pm(t_{n+1/2})\|_{r+1}^2 \right) + \epsilon\nu^* \|\nabla \xi_{n+1/2}^{\pm,h}\|^2. \end{aligned} \quad (3.25)$$

Similarly,

$$\begin{aligned} I_3 &= -\nu^- (\nabla \eta_{n+1/2}^\mp, \nabla \xi_{n+1/2}^{\pm,h}) \\ &\leq \frac{C(\epsilon)(\nu^-)^2 h^{2r}}{\nu^*} \left(\tau_{\max}^3 \int_{t_n}^{t_{n+1}} \|z_{tt}^\mp\|_{r+1}^2 dt + \|z^\mp(t_{n+1/2})\|_{r+1}^2 \right) + \epsilon\nu^* \|\nabla \xi_{n+1/2}^{\pm,h}\|^2. \end{aligned} \quad (3.26)$$

By the Cauchy-Schwarz and Young inequalities, using (3.16) we have

$$\begin{aligned} I_4 &= \nu^+ (\nabla z^\pm(t_{n+1/2}) - \nabla z_{n+1/2}^\pm, \nabla \xi_{n+1/2}^{\pm,h}) \\ &\leq \nu^+ \|\nabla z^\pm(t_{n+1/2}) - \nabla z_{n+1/2}^\pm\| \|\nabla \xi_{n+1/2}^{\pm,h}\| \\ &\leq \frac{C(\epsilon)(\nu^+)^2 \tau_{\max}^3}{\nu^*} \int_{t_n}^{t_{n+1}} \|\nabla z_{tt}^\pm\|^2 dt + \epsilon\nu^* \|\nabla \xi_{n+1/2}^{\pm,h}\|^2, \end{aligned} \quad (3.27)$$

and

$$\begin{aligned} I_5 &= \nu^- (\nabla z^\mp(t_{n+1/2}) - \nabla z_{n+1/2}^\mp, \nabla \xi_{n+1/2}^{\pm,h}) \\ &\leq \nu^- \|\nabla z^\mp(t_{n+1/2}) - \nabla z_{n+1/2}^\mp\| \|\nabla \xi_{n+1/2}^{\pm,h}\| \\ &\leq \frac{C(\epsilon)(\nu^-)^2 \tau_{\max}^3}{\nu^*} \int_{t_n}^{t_{n+1}} \|\nabla z_{tt}^\mp\|^2 dt + \epsilon\nu^* \|\nabla \xi_{n+1/2}^{\pm,h}\|^2. \end{aligned} \quad (3.28)$$

Now we set q^h to be the L^2 -projection of $p^\pm(t_{n+1/2})$, and use the Cauchy-Schwarz inequality, (2.2) and Young's inequality to obtain

$$\begin{aligned} I_6 &= -(p^\pm(t_{n+1/2}) - q^h, \nabla \cdot \xi_{n+1/2}^{\pm,h}) \leq \sqrt{d} \|p^\pm(t_{n+1/2}) - q^h\| \|\nabla \xi_{n+1/2}^{\pm,h}\| \\ &\leq \frac{C(\epsilon)h^{2s+2}}{\nu^*} \|p^\pm(t_{n+1/2})\|_{s+1}^2 + \epsilon\nu^* \|\nabla \xi_{n+1/2}^{\pm,h}\|^2. \end{aligned} \quad (3.29)$$

Using the Cauchy-Schwarz and Poincaré inequalities, (3.17) and Young's inequality we obtain

$$\begin{aligned} I_7 &= -\left(\frac{z^\pm(t_{n+1}) - z^\pm(t_n)}{\tau_n} - z_t^\pm(t_{n+1/2}), \xi_{n+1/2}^{\pm,h} \right) \\ &\leq \frac{C(\epsilon)\tau_{\max}^3}{\nu^*} \int_{t_n}^{t_{n+1}} \|\nabla z_{ttt}^\mp\|^2 dt + \epsilon\nu^* \|\nabla \xi_{n+1/2}^{\pm,h}\|^2. \end{aligned} \quad (3.30)$$

By Holder's inequality and the Sobolev embedding theorem, the Poincaré inequality, using $\nabla B_o = 0$, the approximations (2.6), (2.2) and (3.16), we have

$$\begin{aligned}
I_8 &= \pm \mathcal{N}(B_o, \eta^\pm(t_{n+1/2}), \xi_{n+1/2}^{\pm, h}) \\
&\leq C(\|B_o\| \|B_o\|_1)^{1/2} \|\nabla \eta_{n+1/2}^\pm\| \|\xi_{n+1/2}^{\pm, h}\|_1 \\
&\leq C\|B_o\| \|\nabla \eta_{n+1/2}^\pm\| \|\nabla \xi_{n+1/2}^{\pm, h}\| \\
&\leq Ch^r \|B_o\| (\|z_{n+1/2}^\pm - z^\pm(t_{n+1/2})\|_{r+1} + \|z^\pm(t_{n+1/2})\|_{r+1}) \|\nabla \xi_{n+1/2}^{\pm, h}\| \\
&\leq \frac{C(\epsilon)h^{2r}}{\nu^*} \|B_o\|^2 (\tau_{\max}^3 \int_{t_n}^{t_{n+1}} \|z_{tt}^\pm\|_{r+1}^2 dt + \|z^\pm(t_{n+1/2})\|_{r+1}^2) + \epsilon \nu^* \|\nabla \xi_{n+1/2}^{\pm, h}\|^2,
\end{aligned} \tag{3.31}$$

and

$$\begin{aligned}
I_9 &= \pm \mathcal{N}(B_o, z_{n+1/2}^\pm - z^\pm(t_{n+1/2}), \xi_{n+1/2}^{\pm, h}) \\
&\leq C\|B_o\| \|\nabla z_{n+1/2}^\pm - \nabla z^\pm(t_{n+1/2})\| \|\nabla \xi_{n+1/2}^{\pm, h}\| \\
&\leq \frac{C(\epsilon)\tau_{\max}^3}{\nu^*} \|B_o\|^2 \int_{t_n}^{t_{n+1}} \|\nabla z_{tt}^\pm\|^2 dt + \epsilon \nu^* \|\nabla \xi_{n+1/2}^{\pm, h}\|^2.
\end{aligned} \tag{3.32}$$

Similarly to (3.32) we obtain

$$\begin{aligned}
I_{10} &= \mathcal{N}(z^\mp(t_{n+1/2}), z^\pm(t_{n+1/2}), \xi_{n+1/2}^{\pm, h}) - \mathcal{N}(z_{n+1/2}^\mp, z_{n+1/2}^\pm, \xi_{n+1/2}^{\pm, h}) \\
&\leq \mathcal{N}(z^\mp(t_{n+1/2}) - z_{n+1/2}^\mp, z^\pm(t_{n+1/2}), \xi_{n+1/2}^{\pm, h}) + \mathcal{N}(z_{n+1/2}^\mp, z^\pm(t_{n+1/2}) - z_{n+1/2}^\pm, \xi_{n+1/2}^{\pm, h}) \\
&\leq C\|\nabla(z^\mp(t_{n+1/2}) - z_{n+1/2}^\mp)\| \|\nabla z^\pm(t_{n+1/2})\| \|\nabla \xi_{n+1/2}^{\pm, h}\| \\
&\quad + C\|\nabla z_{n+1/2}^\mp\| \|\nabla(z^\pm(t_{n+1/2}) - z_{n+1/2}^\pm)\| \|\nabla \xi_{n+1/2}^{\pm, h}\| \\
&\leq \frac{C(\epsilon)\tau_{\max}^3}{\nu^*} \left(\|z^\mp\|_{\infty, 1}^2 \int_{t_n}^{t_{n+1}} \|\nabla z_{tt}^\pm\|^2 dt + \|z^\pm\|_{\infty, 1, 1/2}^2 \int_{t_n}^{t_{n+1}} \|\nabla z_{tt}^\mp\|^2 dt \right) \\
&\quad + \epsilon \nu^* \|\nabla \xi_{n+1/2}^{\pm, h}\|^2.
\end{aligned} \tag{3.33}$$

By the skew-symmetriy property (2.7) we can write I_{11} as

$$\begin{aligned}
I_{11} &= \mathcal{N}(z_{n+1/2}^\mp, z_{n+1/2}^\pm, \xi_{n+1/2}^{\pm, h}) - \mathcal{N}(z_{n+1/2}^{\mp, h}, z_{n+1/2}^{\pm, h}, \xi_{n+1/2}^{\pm, h}) \\
&= -\mathcal{N}(\xi_{n+1/2}^{\mp, h}, z_{n+1/2}^\pm, \xi_{n+1/2}^{\pm, h}) - \mathcal{N}(\eta_{n+1/2}^\mp, z_{n+1/2}^\pm, \xi_{n+1/2}^{\pm, h}) - \mathcal{N}(\xi_{n+1/2}^{\mp, h}, \eta_{n+1/2}^\pm, \xi_{n+1/2}^{\pm, h}) \\
&\quad - \mathcal{N}(\eta_{n+1/2}^\mp, \eta_{n+1/2}^\pm, \xi_{n+1/2}^{\pm, h}) - \mathcal{N}(z_{n+1/2}^\mp, \eta_{n+1/2}^\pm, \xi_{n+1/2}^{\pm, h}) = I_{11}^{(1)} + \dots + I_{11}^{(5)}.
\end{aligned}$$

Now we evaluate each term in the right hand side above as follows. By Hölder's inequality, (2.9), Poincaré and Young's inequality we have

$$\begin{aligned}
I_{11}^{(1)} &= -\mathcal{N}(\xi_{n+1/2}^{\mp, h}, z_{n+1/2}^\pm, \xi_{n+1/2}^{\pm, h}) \\
&\leq \epsilon \nu^* \|\nabla \xi_{n+1/2}^{\pm, h}\|^2 + \epsilon \nu^* \|\nabla \xi_{n+1/2}^{\mp, h}\|^2 + \frac{(3(d-1))^{4d/3} C_P^{2(3-d)}}{64(\epsilon \nu^*)^3 d^{7d/3}} \|\nabla z_{n+1/2}^\pm\|^4 \|\xi_{n+1/2}^{\mp, h}\|^2.
\end{aligned} \tag{3.34}$$

Similarly,

$$I_{11}^{(2)} = -\mathcal{N}(\eta_{n+1/2}^\mp, z_{n+1/2}^\pm, \xi_{n+1/2}^{\pm, h}) \tag{3.35}$$

$$\leq \epsilon \nu^* \|\nabla \xi_{n+1/2}^{\pm, h}\|^2 + \frac{C(\epsilon)}{\nu^*} \left(\|\nabla z_{n+1}^{\pm}\|^2 + \|\nabla z_n^{\pm}\|^2 \right) \|\nabla \eta_{n+1/2}^{\mp}\|^2.$$

Using Hölder's inequality, (2.9), Poincaré and Young's inequality, (2.6), (2.2) and the inverse inequality (2.3) we get

$$\begin{aligned} I_{11}^{(3)} &= -\mathcal{N}(\xi_{n+1/2}^{\mp, h}, \eta_{n+1/2}^{\pm}, \xi_{n+1/2}^{\pm, h}) \\ &\leq \frac{(3(d-1))^{d/3}}{d^{7d/12}} C_P^{(3-d)/2} (\|\xi_{n+1/2}^{\mp, h}\| \|\nabla \xi_{n+1/2}^{\mp, h}\|)^{1/2} \|\nabla \eta_{n+1/2}^{\pm}\| \|\nabla \xi_{n+1/2}^{\pm, h}\| \\ &\leq \epsilon \nu^* \|\nabla \xi_{n+1/2}^{\pm, h}\|^2 + \frac{(3(d-1))^{2d/3} C_P^{3-d} C_I (C_A^{1,0})^2}{\epsilon \nu^* d^{7d/6}} \left(1 + \frac{1}{\beta_{\text{is}}}\right)^2 h |z_{n+1/2}^{\pm}|_2 \|\xi_{n+1/2}^{\mp, h}\|^2, \end{aligned} \quad (3.36)$$

also

$$\begin{aligned} I_{11}^{(4)} &= -\mathcal{N}(\eta_{n+1/2}^{\mp}, \eta_{n+1/2}^{\pm}, \xi_{n+1/2}^{\pm, h}) \leq C(\|\nabla \eta_{n+1}^{\mp}\| + \|\nabla \eta_n^{\mp}\|) \|\nabla \eta_{n+1/2}^{\pm}\| \|\nabla \xi_{n+1/2}^{\pm, h}\| \\ &\leq \epsilon \nu^* \|\nabla \xi_{n+1/2}^{\pm, h}\|^2 + \frac{C(\epsilon)}{\nu^*} (\|\nabla z_{n+1}^{\mp}\|^2 + \|\nabla z_n^{\mp}\|^2) \|\nabla \eta_{n+1/2}^{\pm}\|^2, \end{aligned} \quad (3.37)$$

and finally

$$\begin{aligned} I_{11}^{(5)} &= -\mathcal{N}(z_{n+1/2}^{\mp}, \eta_{n+1/2}^{\pm}, \xi_{n+1/2}^{\pm, h}) \leq C(\|\nabla z_{n+1}^{\mp}\| + \|\nabla z_n^{\mp}\|) \|\nabla \eta_{n+1/2}^{\pm}\| \|\nabla \xi_{n+1/2}^{\pm, h}\| \\ &\leq \epsilon \nu^* \|\nabla \xi_{n+1/2}^{\pm, h}\|^2 + \frac{C(\epsilon)}{\nu^*} (\|\nabla z_{n+1}^{\mp}\|^2 + \|\nabla z_n^{\mp}\|^2) \|\nabla \eta_{n+1/2}^{\pm}\|^2. \end{aligned} \quad (3.38)$$

Therefore, we combine (3.34)-(3.38) to obtain

$$\begin{aligned} I_{11} &= \mathcal{N}(z_{n+1/2}^{\mp}, z_{n+1/2}^{\pm}, \xi_{n+1/2}^{\pm, h}) - \mathcal{N}(z_{n+1/2}^{\mp, h}, z_{n+1/2}^{\pm}, \xi_{n+1/2}^{\pm, h}) \\ &\leq \frac{(3(d-1))^{2d/3} C_P^{3-d} C_I (C_A^{1,0})^2}{\epsilon \nu^* d^{7d/6}} \left(1 + \frac{1}{\beta_{\text{is}}}\right)^2 h |z_{n+1/2}^{\pm}|_2 \|\xi_{n+1/2}^{\mp, h}\|^2 \\ &\quad + \frac{(3(d-1))^{4d/3} C_P^{2(3-d)}}{64(\epsilon \nu^*)^3 d^{7d/3}} \|\nabla z_{n+1/2}^{\pm}\|^4 \|\xi_{n+1/2}^{\mp, h}\|^2 \\ &\quad + \frac{C(\epsilon)}{\nu^*} (\|\nabla z_{n+1}^{\pm}\|^2 + \|\nabla z_n^{\pm}\|^2) \|\nabla \eta_{n+1/2}^{\mp}\|^2 \\ &\quad + \frac{C(\epsilon)}{\nu^*} (\|\nabla z_{n+1}^{\mp}\|^2 + \|\nabla z_n^{\mp}\|^2) \|\nabla \eta_{n+1/2}^{\pm}\|^2 + 5\epsilon \nu^* \|\nabla \xi_{n+1/2}^{\pm, h}\|^2 + \epsilon \nu^* \|\nabla \xi_{n+1/2}^{\mp, h}\|^2. \end{aligned} \quad (3.39)$$

Now we use (2.6), (2.2), the triangle inequality and (3.16) to evaluate

$$\|\nabla \eta_{n+1/2}^{\pm}\|^2 \leq Ch^{2r} \|z_{n+1/2}^{\pm}\|_{r+1}^2 \leq Ch^{2r} \tau_{\max}^3 \int_{t_n}^{t_{n+1}} \|z_{tt}^{\pm}\|_{r+1}^2 dt + Ch^{2r} \|z^{\pm}(t_{n+1/2})\|_{r+1}^2,$$

to get

$$\begin{aligned} I_{11} &= \mathcal{N}(z_{n+1/2}^{\mp}, z_{n+1/2}^{\pm}, \xi_{n+1/2}^{\pm, h}) - \mathcal{N}(z_{n+1/2}^{\mp, h}, z_{n+1/2}^{\pm}, \xi_{n+1/2}^{\pm, h}) \\ &\leq \frac{(3(d-1))^{2d/3} C_P^{3-d} C_I (C_A^{1,0})^2}{\epsilon \nu^* d^{7d/6}} \left(1 + \frac{1}{\beta_{\text{is}}}\right)^2 h |z_{n+1/2}^{\pm}|_2 \|\xi_{n+1/2}^{\mp, h}\|^2 \end{aligned} \quad (3.40)$$

$$\begin{aligned}
& + \frac{(3(d-1))^{4d/3} C_P^{2(3-d)}}{64(\epsilon\nu^*)^3 d^{7d/3}} \|\nabla z_{n+1/2}^\pm\|^4 \|\xi_{n+1/2}^{\mp,h}\|^2 + 5\epsilon\nu^* \|\nabla \xi_{n+1/2}^{\pm,h}\|^2 + \epsilon\nu^* \|\nabla \xi_{n+1/2}^{\mp,h}\|^2 \\
& + \frac{C(\epsilon)h^{2r}}{\nu^*} \|\nabla z^\mp\|_{\infty,0}^2 \left(\tau_{\max}^3 \int_{t_n}^{t_{n+1}} \|z_{tt}^\pm\|_{r+1}^2 dt + \|z^\pm(t_{n+1/2})\|_{r+1}^2 \right) \\
& + \frac{C(\epsilon)h^{2r}}{\nu^*} \|\nabla z^\pm\|_{\infty,0}^2 \left(\tau_{\max}^3 \int_{t_n}^{t_{n+1}} \|z_{tt}^\mp\|_{r+1}^2 dt + \|z^\mp(t_{n+1/2})\|_{r+1}^2 \right).
\end{aligned}$$

We combine (3.23)-(3.33) and (3.40) to obtain the following bound for (3.23)

$$\begin{aligned}
& \frac{1}{2\tau_n} (\|\xi_{n+1}^{\pm,h}\|^2 - \|\xi_n^{\pm,h}\|^2) + \nu^+ \|\nabla \xi_{n+1/2}^{\pm,h}\|^2 - \frac{|\nu^-|}{2} (\|\nabla \xi_{n+1/2}^{\mp,h}\|^2 + \|\nabla \xi_{n+1/2}^{\pm,h}\|^2) \\
& + \frac{|\nu^-|}{2} \|\nabla \xi_{n+1/2}^{\mp,h} + \text{sign}(\nu^-) \nabla \xi_{n+1/2}^{\pm,h}\|^2 - 15\epsilon\nu^* \|\nabla \xi_{n+1/2}^{\pm,h}\|^2 - \epsilon\nu^* \|\nabla \xi_{n+1/2}^{\mp,h}\|^2 \\
& \leq \frac{(3(d-1))^{2d/3} C_P^{3-d} C_I(C_A^{1,0})^2}{\epsilon\nu^* d^{7d/6}} \left(1 + \frac{1}{\beta_{\text{is}}}\right)^2 h |z_{n+1/2}^\pm|_2 \|\xi_{n+1/2}^{\mp,h}\|^2 \\
& + \frac{(3(d-1))^{4d/3} C_P^{2(3-d)}}{64(\epsilon\nu^*)^3 d^{7d/3}} \|\nabla z_{n+1/2}^\pm\|^4 \|\xi_{n+1/2}^{\mp,h}\|^2 + \frac{C(\epsilon)h^{2r+2}}{\tau_n \nu^*} \int_{t_n}^{t_{n+1}} \|z^\pm\|_{r+1}^2 dt \\
& + \frac{C(\epsilon)(\nu^+)^2 h^{2r}}{\nu^*} \left(\tau_{\max}^3 \int_{t_n}^{t_{n+1}} \|z_{tt}^\pm\|_{r+1}^2 dt + \|z^\pm(t_{n+1/2})\|_{r+1}^2 \right) \\
& + \frac{C(\epsilon)(\nu^-)^2 h^{2r}}{\nu^*} \left(\tau_{\max}^3 \int_{t_n}^{t_{n+1}} \|z_{tt}^\mp\|_{r+1}^2 dt + \|z^\mp(t_{n+1/2})\|_{r+1}^2 \right) \\
& + \frac{C(\epsilon)(\nu^-)^2 \tau_{\max}^3}{\nu^*} \left(\int_{t_n}^{t_{n+1}} \|\nabla z_{tt}^\mp\|^2 dt + \int_{t_n}^{t_{n+1}} \|\nabla z_{tt}^\mp\|^2 dt \right) + \frac{C(\epsilon)h^{2s+2}}{\nu^*} \|p^\pm(t_{n+1/2})\|_{s+1}^2 \\
& + \frac{C(\epsilon)\tau_{\max}^3}{\nu^*} \int_{t_n}^{t_{n+1}} \|\nabla z_{ttt}^\mp\|^2 dt + \frac{C(\epsilon)\tau_{\max}^3}{\nu^*} \|B_\circ\|^2 \int_{t_n}^{t_{n+1}} \|\nabla z_{tt}^\pm\|^2 dt \\
& + \frac{C(\epsilon)h^{2r}}{\nu^*} \|B_\circ\|^2 \left(\tau_{\max}^3 \int_{t_n}^{t_{n+1}} \|z_{tt}^\pm\|_{r+1}^2 dt + \|z^\pm(t_{n+1/2})\|_{r+1}^2 \right) \\
& + \frac{C(\epsilon)\tau_{\max}^3}{\nu^*} \left(\|z^\mp\|_{\infty,1}^2 \int_{t_n}^{t_{n+1}} \|\nabla z_{tt}^\pm\|^2 dt + \|z^\pm\|_{\infty,1,1/2}^2 \int_{t_n}^{t_{n+1}} \|\nabla z_{tt}^\mp\|^2 dt \right) \\
& + \frac{C(\epsilon)h^{2r}}{\nu^*} \|\nabla z^\mp\|_{\infty,0}^2 \left(\tau_{\max}^3 \int_{t_n}^{t_{n+1}} \|z_{tt}^\pm\|_{r+1}^2 dt + \|z^\pm(t_{n+1/2})\|_{r+1}^2 \right) \\
& + \frac{C(\epsilon)h^{2r}}{\nu^*} \|\nabla z^\pm\|_{\infty,0}^2 \left(\tau_{\max}^3 \int_{t_n}^{t_{n+1}} \|z_{tt}^\mp\|_{r+1}^2 dt + \|z^\mp(t_{n+1/2})\|_{r+1}^2 \right).
\end{aligned}$$

Now adding the two relations above, and summing over n from 0 to $N-1$ yields

$$\begin{aligned}
& \left[1 - \left(\frac{C_1^* h Z_{N-1}^1}{\epsilon} + \frac{C_2^* Z_{N-1}^2}{\epsilon^3} \right) \tau_{N-1} \right] (\|\xi_N^{+,h}\|^2 + \|\xi_N^{-,h}\|^2) \\
& + 2\nu^* (1 - 16\epsilon) \sum_{n=1}^{N-1} \tau_n (\|\nabla \xi_{n+1/2}^{+,h}\|^2 + \|\nabla \xi_{n+1/2}^{-,h}\|^2) \\
& \leq \sum_{n=1}^{N-1} \left(\frac{C_1^* h Z_n^1}{\epsilon} + \frac{C_2^* Z_n^2}{\epsilon^3} \right) \tau_n (\|\xi_n^{+,h}\|^2 + \|\xi_n^{-,h}\|^2) + C(\epsilon) F(h^{2r}, h^{2s+2}, \tau_{\max}^4, \|B_\circ\|^2).
\end{aligned} \tag{3.42}$$

Here we impose the positivity conditions

$$\begin{aligned} 1 - \left(\frac{C_1^* h Z_{N-1}^1}{\epsilon} + \frac{C_2^* Z_{N-1}^2}{\epsilon^3} \right) \tau_{N-1} &> 0, \\ 1 - 16\epsilon &> 0, \end{aligned}$$

which imply the time step restrictions (3.19). The discrete Grönwall inequality [24, p. 369] applied to (3.42) gives

$$\begin{aligned} &(\|\xi_N^{+,h}\|^2 + \|\xi_N^{-,h}\|^2) + \nu^* \sum_{n=1}^{N-1} \tau_n (\|\nabla \xi_{n+1/2}^{+,h}\|^2 + \|\nabla \xi_{n+1/2}^{-,h}\|^2) \\ &\leq C \exp \left(C \sum_{n=1}^{N-1} (C_1^* h Z_n^1 + C_2^* Z_n^2) \tau_n \right) F(h^{2r}, h^{2s+2}, \tau_{\max}^4, \|B_o\|^2). \end{aligned} \quad (3.43)$$

We use the triangle inequality, (2.6), (2.2), (3.16) and (3.43) to obtain

$$\|e_N^\pm\|^2 \leq 2\|\xi_N^{\pm,h}\|^2 + 2\|\eta_N^\pm\|^2 \leq 2\|\xi_N^{\pm,h}\|^2 + Ch^{2r} \|z^\pm\|_{\infty, r+1}^2, \quad (3.44)$$

and

$$\begin{aligned} &\nu^* \sum_{n=1}^{N-1} \tau_n \|\nabla(e_{n+1}^\pm + e_n^\pm)/2\|^2 \leq 2\nu^* \sum_{n=1}^{N-1} \tau_n (\|\nabla \xi_{n+1/2}^{\pm,h}\|^2 + \|\nabla \eta_{n+1/2}^\pm\|^2) \\ &\leq 2\nu^* \sum_{n=1}^{N-1} \tau_n \|\nabla \xi_{n+1/2}^{\pm,h}\|^2 + C\nu^* h^{2r} \tau_n \sum_{n=1}^{N-1} (\|z_{n+1/2}^\pm - z^\pm(t_{n+1/2})\|_{r+1}^2 + \|z^\pm(t_{n+1/2})\|_{r+1}^2) \\ &\leq 2\nu^* \sum_{n=1}^{N-1} \tau_n \|\nabla \xi_{n+1/2}^{\pm,h}\|^2 + C\nu^* h^{2r} (\tau_{\max}^4 \|z^\pm\|_{2, r+1}^2 + \|z^\pm\|_{2, r+1, 1/2}^2). \end{aligned}$$

Finally, we apply (2.6), (2.2) in (3.44) and use (3.42) to derive (3.20). \square

4. Time Adaptivity. To construct the time adaptive mechanism for the fully-coupled implicit monolithic method (1.4) with the BE partitioned iteration (1.6) (PIM algorithm), we estimate its local truncation error (LTE) by the fully-explicit two-step AB2-like scheme¹ and adopt the improved time step controller proposed in [22] to adjust time steps. The AB2-like scheme for the ordinary differential equation $y' = g(t, y)$ is

$$\begin{aligned} y_{n+1}^{\text{AB2-like}} = y_n + \frac{t_{n+1} - t_n}{2(t_{n-1/2} - t_{n-3/2})} &\left[(t_{n+1} + t_n - 2t_{n-3/2}) g^{\text{Mid}}(t_{n-1/2}, y_{n-1/2}) \right. \\ &\left. - (t_{n+1} + t_n - 2t_{n-1/2}) g^{\text{Mid}}(t_{n-3/2}, y_{n-3/2}) \right], \end{aligned} \quad (4.1)$$

where $g^{\text{Mid}}(t_{n-1/2}, y_{n-1/2})$ and $g^{\text{Mid}}(t_{n-3/2}, y_{n-3/2})$ are calculated by the midpoint rule at time nodes t_n, t_{n-1} and t_{n-1}, t_{n-2} , respectively, i.e.,

$$g^{\text{Mid}}(t_{n-1/2}, y_{n-1/2}) = \frac{y_n - y_{n-1}}{\tau_{n-1}}, \quad g^{\text{Mid}}(t_{n-3/2}, y_{n-3/2}) = \frac{y_{n-1} - y_{n-2}}{\tau_{n-2}}.$$

¹The derivation of scheme is similar to that of two-step Adam-Bashforth (AB2) scheme, hence we call it AB2-like scheme.

From (4.1) we see that $y_{n+1}^{\text{AB2-like}}$ is a certain interpolant of the previous three midpoint rule solutions $\{y_n, y_{n-1}, y_{n-2}\}$. Hence, the AB2-like scheme (4.1) is fully explicit. We refer to [8] for the derivation of the explicit AB2-like scheme (4.1) and the following estimator of LTE \hat{T}_{n+1} of the midpoint rule by AB2-like scheme

$$\begin{aligned}\hat{T}_{n+1} &= \frac{1/24}{\mathcal{R}^{(n)} - 1/24} (y_{n+1}^{\text{Mid}} - y_{n+1}^{\text{AB2-like}}), \\ \mathcal{R}^{(n)} &= \frac{1}{12} \left[2 + \frac{3}{\rho_n} \left(1 + \frac{1}{2\rho_{n-1}} \right) \left(1 + \frac{1}{2\rho_n} \right) + \frac{3}{2\rho_n} \left(1 + \frac{1}{\rho_n} + \frac{1}{2} \frac{1}{\rho_{n-1}} \frac{1}{\rho_n} \right) \right],\end{aligned}$$

and $\rho_n = \tau_n / \tau_{n-1}$ denotes the ratio of consecutive time steps. The AB2-like solutions for the MHD system in Elsässer variables (1.3) at time t_{n+1} is

$$\begin{aligned}z_{n+1}^{\pm, \text{AB2-like}} &= z_n^{\pm} + \frac{t_{n+1} - t_n}{2(t_{n-1/2} - t_{n-3/2})} \left[(t_{n+1} + t_n - 2t_{n-3/2}) \frac{z_n^{\pm} - z_{n-1}^{\pm}}{\tau_{n-1}} \right. \\ &\quad \left. - (t_{n+1} + t_n - 2t_{n-1/2}) \frac{z_{n-1}^{\pm} - z_{n-2}^{\pm}}{\tau_{n-2}} \right],\end{aligned}\quad (4.2)$$

where $\{z_n^{\pm}, z_{n-1}^{\pm}, z_{n-2}^{\pm}\}$ are three previous solutions by the PIM algorithm in (1.4). The corresponding estimator of LTE for the PIM algorithm (1.4) is

$$\hat{T}_{n+1} = \max \left\{ \frac{|1/24| \|z_{n+1}^+ - z_{n+1}^{+, \text{AB2-like}}\|}{|\mathcal{R}^{(n)} - 1/24| \|z_{n+1}^+\|}, \frac{|1/24| \|z_{n+1}^- - z_{n+1}^{-, \text{AB2-like}}\|}{|\mathcal{R}^{(n)} - 1/24| \|z_{n+1}^-\|} \right\}. \quad (4.3)$$

The improved time step controller is

$$\tau_{n+1} = \tau_n \cdot \min \left\{ 1.5, \max \left\{ 0.2, \kappa (\text{To1} / \|\hat{T}_{n+1}\|)^{\frac{1}{3}} \right\} \right\}, \quad (4.4)$$

where $\kappa \in (0, 1]$ is the safety factor and To1 is the required tolerance for the LTE. We note that, for efficiency, the step controller in (4.4) increases the step size if the estimator for LTE \hat{T}_{n+1} is small with respect to To1 . Meanwhile, for the robustness of computations, the controller bounds the new time step τ_{n+1} between $0.2\tau_n$ and $1.5\tau_n$. We summarize the time adaptivity mechanism in the following algorithm.

Algorithm 1: Adaptivity of the PIM algorithm (1.4)

Input: tolerance To1 , previous solutions $z_n^\pm, z_{n-1}^\pm, z_{n-2}^\pm$ by the PIM algorithm in (1.4), current time step τ_n , two previous time step τ_{n-1}, τ_{n-2} , safety factor κ ;

compute the current solution $z_{n+1}^{\pm, \text{PIM}}$ and p_{n+1}^\pm by the refactorization process ;

compute the AB2-like solution $z_{n+1}^{\pm, \text{AB2-like}}$ by (4.2) ;

use $\tau_n, \tau_{n-1}, \tau_{n-2}$ to update ρ_n, ρ_{n-1} ;

compute \hat{T}_{n+1} by (4.3) ; // relative estimator

if $\hat{T}_{n+1} < \text{To1}$ **then**

$z_{n+1}^\pm \leftarrow z_{n+1}^{\pm, \text{PIM}}$; // accept the result

$\tau_{n+1} \leftarrow \tau_n \cdot \min \{1.5, \max \{0.2, \kappa (\frac{\text{To1}}{\hat{T}_{n+1}})^{1/3}\}\}$; // adjust step by (4.4)

else

// adjust current step to recompute

$\tau_n \leftarrow \tau_n \cdot \min \{1.5, \max \{0.2, \kappa (\frac{\text{To1}}{\hat{T}_{n+1}})^{1/3}\}\}$;

5. Numerical Tests. For all numerical tests, we use the Taylor-Hood($\mathbb{P}2 - \mathbb{P}1$) finite element space for spatial discretization and software Freefem++ for programming. We apply the PIM algorithm (1.4) to all numerical tests in this section and compare it with another commonly-used algorithm:

The constant time-stepping second order BDF2-AB2 method [30]

$$\begin{cases} \frac{3z_{n+1}^\pm - 4z_n^\pm + z_{n-1}^\pm}{\tau} \mp (B_\circ \cdot \nabla) z_{n+1}^\pm + ((2z_n^\mp - z_{n-1}^\mp) \cdot \nabla) z_{n+1}^\pm \\ \quad - \nu^+ \Delta z_{n+1}^\pm - \nu^- \Delta (2z_n^\mp - z_{n-1}^\mp) + \nabla p_{n+1}^\pm = 0, \\ \nabla \cdot z_{n+1}^\pm = 0, \end{cases} \quad (5.1)$$

where $\tau > 0$ is the constant time step size. The stopping criterion for the k -th iteration in (1.6) is

$$\|z_{(k)}^\pm - z_{(k-1)}^\pm\| / \|z_{(k)}^\pm\| \leq \text{To1},$$

where To1 is the required tolerance.

5.1. Electrically Conducting 2D Travelling Wave. In this section we verify the rate of convergence of constant time-stepping PIM algorithm on an electrically conducting two-dimensional travelling wave problem [40] on the domain $\Omega = [0.5, 1.5]^2$. The exact solutions (in Elsässer variables) are

$$\begin{aligned} z^+ &= \begin{bmatrix} \frac{3}{4} + \frac{1}{4} \cos(2\pi(x-t)) \sin(2\pi(x-t)) e^{-8\pi^2 \nu t} + \frac{1}{10} (y+1)^2 e^{\nu_m t} \\ -\frac{1}{4} \sin(2\pi(x-t)) \cos(2\pi(x-t)) e^{-8\pi^2 \nu t} + \frac{1}{10} (x+1)^2 e^{\nu_m t} \end{bmatrix}, \\ z^- &= \begin{bmatrix} \frac{3}{4} + \frac{1}{4} \cos(2\pi(x-t)) \sin(2\pi(x-t)) e^{-8\pi^2 \nu t} - \frac{1}{10} (y+1)^2 e^{\nu_m t} \\ -\frac{1}{4} \sin(2\pi(x-t)) \cos(2\pi(x-t)) e^{-8\pi^2 \nu t} - \frac{1}{10} (x+1)^2 e^{\nu_m t} \end{bmatrix}, \\ p &= -\frac{1}{64} (\cos(4\pi(x-t)) + \cos(4\pi(y-t))) e^{-16\pi^2 \nu t}. \end{aligned} \quad (5.2)$$

We set $\nu = \nu_m = 2.5 \times 10^{-4}$, the time step $\Delta t = h$, and the required tolerance $\text{To1} = 1.e-6$ for the convergence of the iterations, at each time step. We test over three

values of B_o : $(0,0)$, $(1,1)$, $(10,10)$, and simulate the problem over time interval $[0,1]$. The initial conditions and boundary conditions are given by the exact solutions. The results of the PIM algorithm (1.4), and the BDF2-AB2 algorithm (5.1) are presented in Tables 5.1 to 5.3. Both algorithms have the second-order convergence rate in L^2 -norm for $B_o = (1,1), (10,10)$. Moreover, the PIM algorithm (1.4) obtains smaller errors for small magnitude of B_o while BDF2-AB2 algorithm (5.1) loses the order of accuracy for the special case of $B_o = (0,0)$.

PIM algorithm					
$\Delta t = h$	$\ z^+ - z^{+,h}\ _{\infty,0}$	Rate	$\ z^- - z^{-,h}\ _{\infty,0}$	Rate	Average iteration
1/16	1.6803e-2		2.5740e-2		9.31
1/32	2.2706e-3	2.8876	5.9990e-3	2.1012	6.19
1/64	5.3284e-4	2.0913	1.4732e-3	2.0258	4.12
1/128	1.3197e-4	2.0135	3.6695e-4	2.0053	3.02
BDF2-AB2 algorithm					
$\Delta t = h$	$\ z^+ - z^{+,h}\ _{\infty,0}$	Rate	$\ z^- - z^{-,h}\ _{\infty,0}$	Rate	
1/16	4.2726e-2		6.5633e-2		
1/32	1.0623e-2	2.0079	2.2256e-2	1.5602	
1/64	9.7834e-3	0.1188	7.9360e-3	1.4877	
1/128	5.0295e-3	0.9600	3.2317e-3	1.2961	

Table 5.1: Error and rate of convergence with $B_o = (0,0)$

PIM algorithm					
$\Delta t = h$	$\ z^+ - z^{+,h}\ _{\infty,0}$	Rate	$\ z^- - z^{-,h}\ _{\infty,0}$	Rate	Average iteration
1/16	1.0656e-2		1.5860e-2		9.44
1/32	2.0089e-3	2.4072	3.3290e-3	2.2523	6.09
1/64	5.1407e-4	1.9663	7.9070e-4	2.0739	4.05
1/128	1.2962e-4	1.9877	1.9466e-4	2.0739	3.01
BDF2-AB2 algorithm					
$\Delta t = h$	$\ z^+ - z^{+,h}\ _{\infty,0}$	Rate	$\ z^- - z^{-,h}\ _{\infty,0}$	Rate	
1/16	2.5927e-2		4.0365e-2		
1/32	5.1292e-3	2.3376	1.0111e-2	1.9972	
1/64	1.2879e-3	1.9937	2.4751e-3	2.0304	
1/128	3.2148e-4	2.0023	6.0824e-4	2.0247	

Table 5.2: Error and rate of convergence with $B_o = (1,1)$

PIM algorithm					
$\Delta t = h$	$\ z^+ - z^{+,h}\ _{\infty,0}$	Rate	$\ z^- - z^{-,h}\ _{\infty,0}$	Rate	Average iteration
1/16	4.0128e-3		3.7020e-3		7.00
1/32	1.0391e-3	2.0952	1.0789e-3	2.1519	5.91
1/64	3.6672e-4	2.2101	3.5414e-4	2.1153	3.75
1/128	1.1268e-4	1.9066	1.1073e-4	1.8706	3.02
BDF2-AB2 algorithm					
$\Delta t = h$	$\ z^+ - z^{+,h}\ _{\infty,0}$	Rate	$\ z^- - z^{-,h}\ _{\infty,0}$	Rate	
1/16	7.2273e-3		5.6705e-3		
1/32	1.0877e-3	2.7322	1.0801e-3	2.3923	
1/64	1.9431e-4	2.4849	2.2144e-4	2.2862	
1/128	4.7211e-5	2.0412	5.5349e-5	2.0003	

Table 5.3: Error and rate of convergence with $B_o = (10, 10)$

5.2. Hartmann Flows. The 2D Hartmann Flows problem on the domain $\Omega = [0, L] \times [-1, 1]$ has the following exact solutions [19]

$$\begin{aligned}
u &= (u_1(y), 0), & B &= (b_1(y), M), & B_o &= (0, M), \\
u_1(y) &= \frac{G}{\nu \cdot Ha \cdot \tanh(Ha)} \left(1 - \frac{\cosh(y \cdot Ha)}{\cosh(Ha)} \right), \\
b_1(y) &= \frac{G}{S} \left(\frac{\sinh(y \cdot Ha)}{\sinh(Ha)} - y \right), & p(x, y) &= -Gx - \frac{1}{2} S b_1^2(y),
\end{aligned} \tag{5.3}$$

where $M > 0$ is the parameter of external magnetic field, $Ha > 0$ is the Hartmann number and $L, G, S > 0$ are other parameters of the problems. We first verify the convergence rate of PIM algorithm by setting $L = 6$, $G = S = 1$, $Ha = 5$, $\nu = 0.1 = \nu_m$ and required tolerance $\text{To1} = 1.e - 6$ for the fixed point iteration. It is easy to check that the MHD equations in (1.1) with steady solutions in (5.3) is a conservative system. We simulate the problem by the constant time-stepping PIM algorithm with four values of B_o : $(0, 1)$, $(0, 10)$, $(0, 100)$, $(0, 1000)$ over the time interval $[0, 1]$ to confirm the rate of convergence. The two initial solutions and boundary conditions are compatible with the exact solutions in (5.3). From Table 5.4, we observe that the constant time-stepping PIM algorithm has achieved a super convergence rate in L^2 -norm. For the long-time conservation, we compare the PIM algorithm with the BDF2-AB2 algorithm in (5.1) over the time interval $[0, 10]$. We set the diameter $h = L/128$, and the constant time step $\Delta t = 1/128$. From Figures 5.1(a) and 5.1(b), we see that the performance of the BDF2-AB2 algorithm is slightly better than that of the PIM algorithm for a small value of M ($M = 1, 10$) in terms of kinetic energy \mathcal{E}_n . However, as the value of M increases, we find that the results of the two algorithms are very close: the error of the PIM algorithm oscillates around that of the BDF2-AB2 algorithm in Figures 5.1(c) and 5.1(d). We observe similar situations for the error of cross helicity \mathcal{H}_{C_n} in Figure 5.2.

$B_o = (0, 1)$					
$\Delta t = h$	$\ z^+ - z^{+,h}\ _{\infty,0}$	Rate	$\ z^- - z^{-,h}\ _{\infty,0}$	Rate	Average iteration
1/16	3.5146e-3		3.5166e-3		2.87
1/32	4.2923e-4	3.0336	4.2927e-4	3.0343	2
1/64	5.1377e-5	3.0625	5.1377e-5	3.0627	1.37
1/128	5.7723e-5	3.2866	6.0922e-5	3.3215	1
$B_o = (0, 10)$					
$\Delta t = h$	$\ z^+ - z^{+,h}\ _{\infty,0}$	Rate	$\ z^- - z^{-,h}\ _{\infty,0}$	Rate	Average iteration
1/16	8.8998e-3		8.9317e-3		3
1/32	7.8380e-4	3.5052	7.8431e-4	3.5094	2
1/64	6.7809e-5	3.5309	6.7806e-5	3.5319	1.89
1/128	6.8948e-6	3.2979	6.8948e-6	3.2978	1
$B_o = (0, 100)$					
$\Delta t = h$	$\ z^+ - z^{+,h}\ _{\infty,0}$	Rate	$\ z^- - z^{-,h}\ _{\infty,0}$	Rate	Average iteration
1/16	3.5855e-2		3.5794e-2		3.07
1/32	4.9008e-3	2.8711	4.9041e-3	2.8676	2.19
1/64	4.4118e-4	3.4736	4.4140e-4	3.4738	2
1/128	3.1643e-5	3.8014	3.1652e-5	3.8017	2
$B_o = (0, 1000)$					
$\Delta t = h$	$\ z^+ - z^{+,h}\ _{\infty,0}$	Rate	$\ z^- - z^{-,h}\ _{\infty,0}$	Rate	Average iteration
1/16	6.5272e-2		6.5278e-2		3
1/32	1.2988e-2	2.3293	1.2982e-2	2.3301	3
1/64	2.0417e-3	2.6693	2.0417e-3	2.6686	2
1/128	2.5951e-4	2.9759	2.5959e-4	2.9755	2

Table 5.4: Error and rate of convergence for PIM

5.3. Adaptive Test. In this subsection, we will show that the adaptive algorithm (Algorithm (1)) has certain advantages over the corresponding constant time-stepping algorithm in one highly stiff test problems. We revise the Hartmann flow problem in (5.3) by multiplying the exact solution (5.3) with the following time dependent function

$$G(t) = e^{g_1(t)} [\cos(g_2(t)) + \sin(g_2(t))], \quad t_0 \leq t \leq T,$$

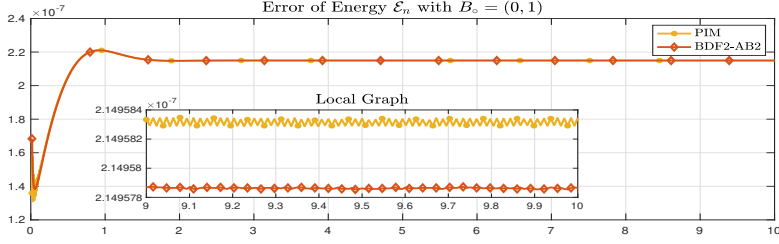
$$\begin{cases} g_1(t) = 10^\omega(t + 2e^{-t} - 2), \\ g_2(t) = 10^\omega(1 - e^{-t} - te^{-1}). \end{cases}$$

Here $G(t)$ is the first component of the solution vector to an extremely stiff ordinary differential system proposed by Lindberg [32]. The exact solutions of the revised Hartmann flow problem on $\Omega = [0, L] \times [-1, 1]$ become

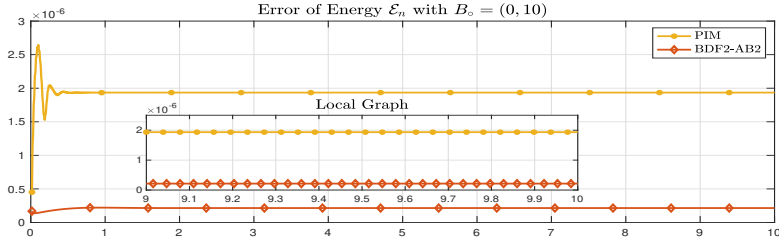
$$u = (u_1(y), 0), \quad B = (b_1(y), M), \quad B_o = (0, M), \quad (5.4)$$

$$u_1(y) = \frac{G}{\nu \cdot Ha \cdot \tanh(Ha)} \left(1 - \frac{\cosh(y \cdot Ha)}{\cosh(Ha)}\right) G(t),$$

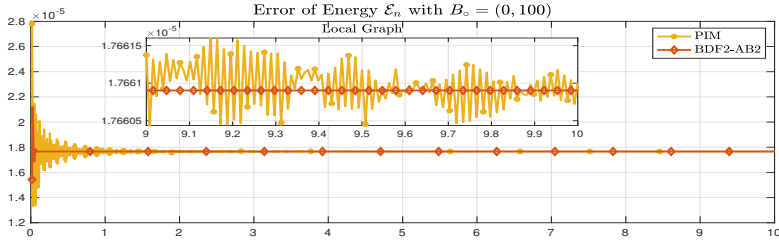
$$b_1(y) = \frac{G}{S} \left(\frac{\sinh(y \cdot Ha)}{\sinh(Ha)} - y\right) G(t), \quad p(x, y) = \left(-Gx - \frac{1}{2} S b_1^2(y)\right) G(t).$$



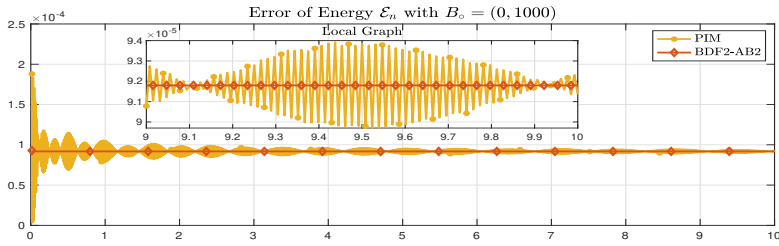
(a) Error of $\mathcal{E}_n = \frac{1}{2}(\|u\|^2 + \|B\|^2)$ with $B_o = (0, 1)$



(b) Error of $\mathcal{E}_n = \frac{1}{2}(\|u\|^2 + \|B\|^2)$ with $B_o = (0, 10)$

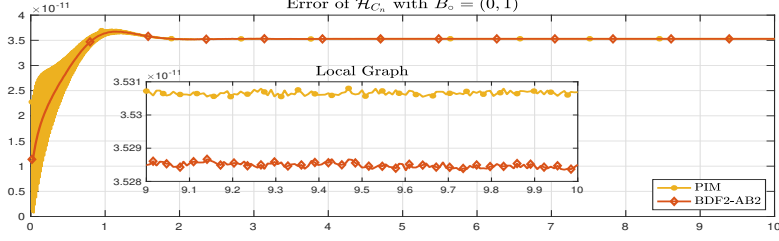


(c) Error of $\mathcal{E}_n = \frac{1}{2}(\|u\|^2 + \|B\|^2)$ with $B_o = (0, 100)$

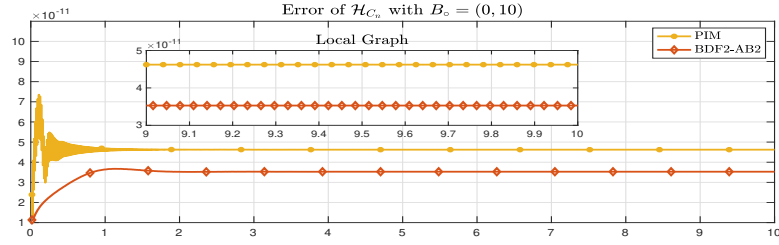


(d) Error of $\mathcal{E}_n = \frac{1}{2}(\|u\|^2 + \|B\|^2)$ with $B_o = (0, 1000)$

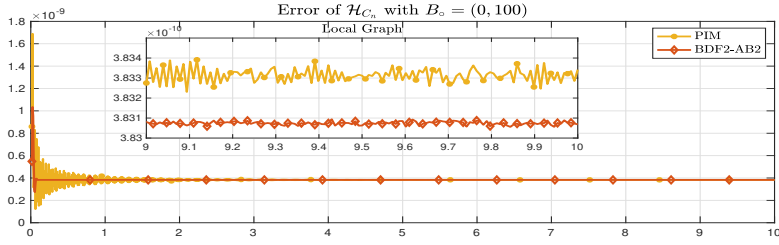
Fig. 5.1: The performance of the BDF2-AB2 algorithm is a slightly better than that of the PIM algorithm for a small value of M ($M = 1, 10$) in terms of kinetic energy \mathcal{E}_n . However, as the value of M increases, we find that the results of the two algorithms are very close: the error of the PIM algorithm oscillates around that of the BDF2-AB2 algorithm.



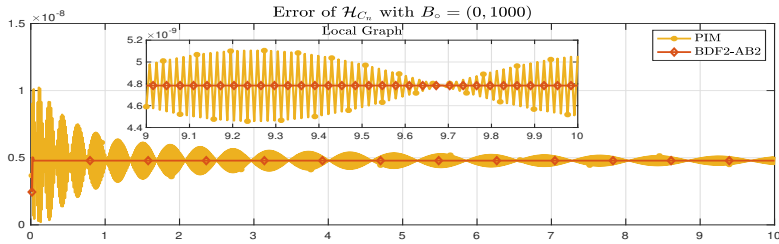
(a) Error of \mathcal{H}_{C_n} with $B_o = (0, 1)$



(b) Error of \mathcal{H}_{C_n} with $B_o = (0, 10)$



(c) Error of \mathcal{H}_{C_n} with $B_o = (0, 100)$



(d) Error of \mathcal{H}_{C_n} with $B_o = (0, 1000)$

Fig. 5.2: The error in the cross helicity \mathcal{H}_{C_n} behaves similarly to the errors in the kinetic energy, for both algorithms.

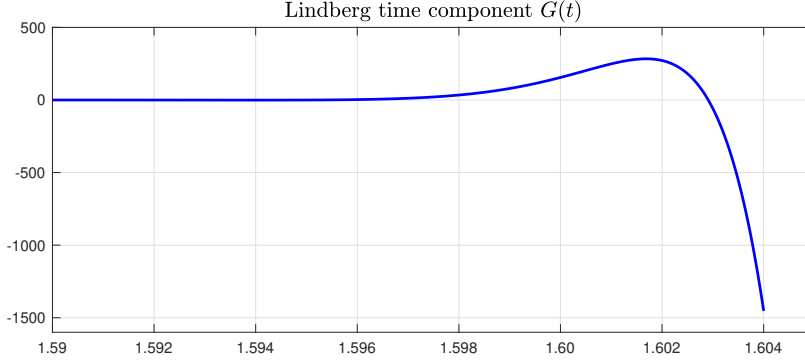
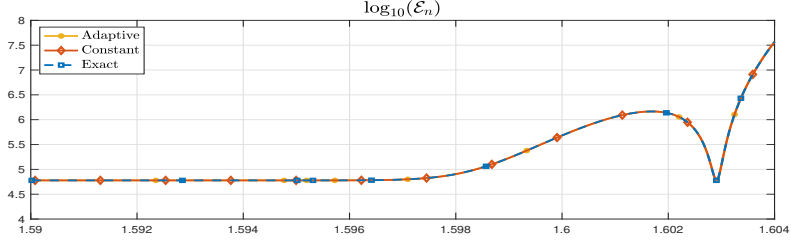


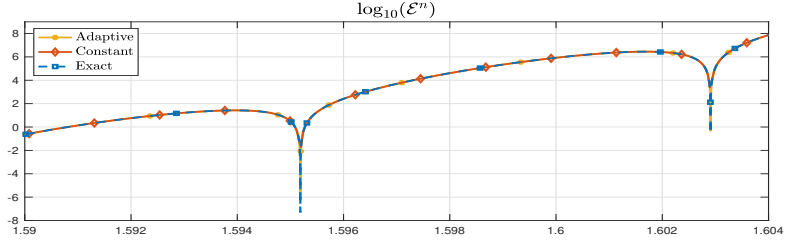
Fig. 5.3: Time component function proposed by Lindberg

We set the parameters $L = 6$, $G = S = 1$, $Ha = 5$, $M = 100$, $\nu = 0.1 = \nu_m$, $\omega = 3.1$ and simulate the problem over the time interval $[1.59, 1.604]$. Figure 5.3 displays the extreme stiffness of $G(t)$: $G(t)$ increases rapidly from 0 ($t = 1.596$) to 300 ($t = 1.6015$) and then declines sharply to -1400 ($t = 1.604$). We set the diameter $h = L/80$, required tolerance $\text{To1} = 1.e - 4$ and the safety factor $\kappa = 0.95$. The maximum time step is $\tau_{\max} = 1.e - 4$ for stability and the minimum time step $\tau_{\min} = 1.e - 6$ for efficiency. Two initial time steps are selected to be the same as τ_{\min} for initial time accuracy. Initial conditions, boundary conditions and source functions are derived from the exact solutions. We verify the accuracy of the adaptive algorithm (Algorithm (1)) by computing the error of energy in u, B and the error of energy in the Elsässer variables. We also apply the corresponding constant time-stepping algorithms with the same number of time steps (342 steps) to confirm the efficiency of the time adaptivity in extremely stiff problems.

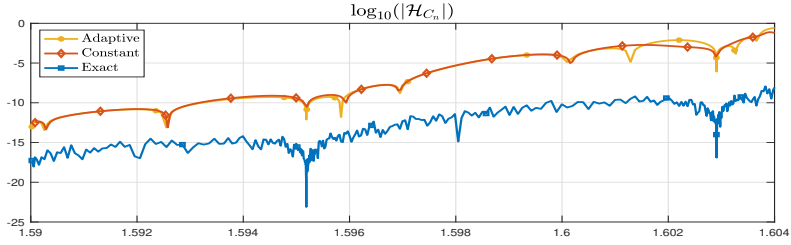
From Figures 5.4(a) and 5.4(b), we observe that both algorithms obtain the true pattern in kinetic energy (KE) and kinetic energy in Elsässer variables, even on the exceedingly stiff regime time range ($t \in [1.603, 1.604]$). Meanwhile, Figure 5.4(c) shows that the cross helicity of both algorithms keeps at a higher level but displays an increasing trend, which is consistent with that of the exact solutions. Figure 5.5 confirms that the adaptive algorithm outperforms the corresponding constant time-stepping algorithm due to a much smaller error in kinetic energy at the end ($t = 1.604$). Figures 5.6(a) and 5.6(b) demonstrate that the adaptive algorithm (Algorithm (1)) balances the efficiency and accuracy: the estimator of LTE \hat{T}_{n+1} at most time steps is close to but below the required tolerance $\text{To1} = 1.e - 4$, so that k_n at most time steps is above τ_{\min} . The adaptive algorithm (Algorithm (1)) assigns more time steps to the highly stiff part ($t \geq 1.602$), which results in a smaller error in the kinetic energy at the end ($t = 1.604$). From Figure 5.6(c), both algorithms have relatively high computational costs on the extremely stiff time range ($t \in [1.603, 1.604]$) since the number of iterations at each time step increases from 2 to 6.



(a) log-plot of KE

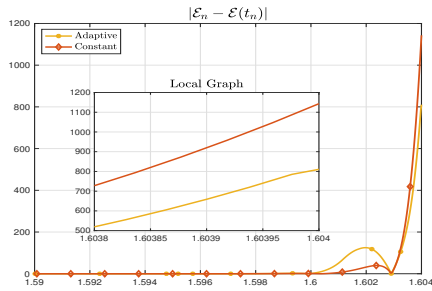


(b) log-plot of KE in Elsässer variables

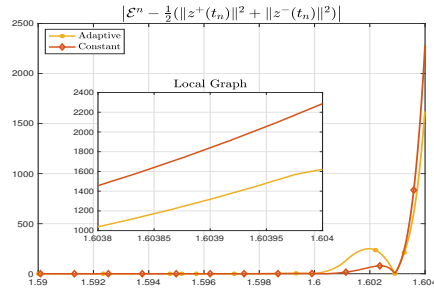


(c) log-plot of cross helicity

Fig. 5.4: Both algorithms obtain the true pattern in kinetic energy (KE) and kinetic energy in Elsässer variables, even on the extremely stiff time range. Meanwhile cross helicity of both algorithms keep at a higher level but display an increasing trend, which is consistent with that of the exact solutions.

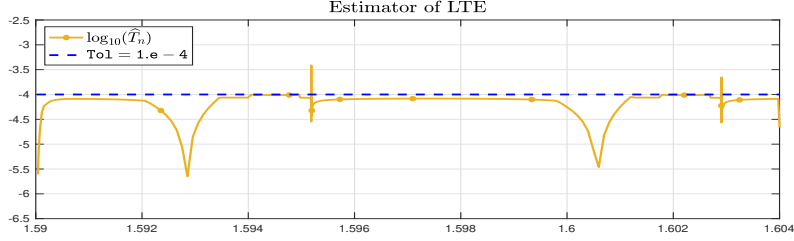


(a) Error of KE

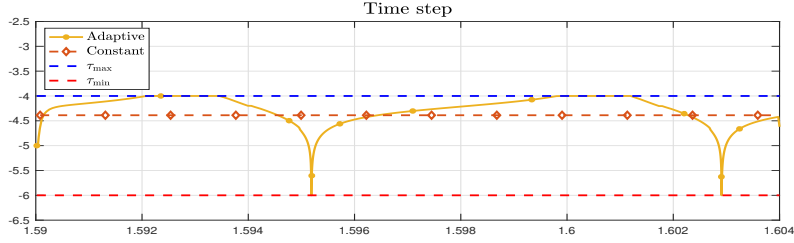


(b) Error of KE in Elsässer variables

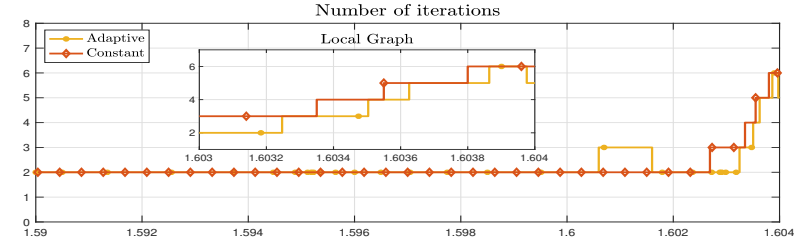
Fig. 5.5: The adaptive algorithm outperforms the corresponding constant time-stepping algorithm due to much smaller error in kinetic energy at the end ($t = 1.604$).



(a) Estimator of LTE



(b) Time step size



(c) Number of iteration at each time step

Fig. 5.6: The adaptive algorithm (Algorithm (1)) balances the efficiency and accuracy: the estimator of LTE \hat{T}_{n+1} at most time steps is close to, but below the required tolerance $\text{Tol} = 1.e-4$, so that τ_n at most time steps is above τ_{\min} . The adaptive algorithm (Algorithm (1)) assigns more time steps to the highly stiff part ($t \geq 1.602$), which results in a smaller error in kinetic energy at the end ($t = 1.604$). Both algorithms have relatively high computational costs on the extremely stiff time range ($t \in [1.603, 1.604]$) since the number of iterations at each time step increases from 2 to 6.

Acknowledgement. We thank Professor Michael Neilan for many helpful discussions. Catalin Trenchea is partially supported by the National Science Foundation under grant DMS-2208220.

6. Conclusion. In this paper we developed an efficient fully-coupled implicit monolithic method for the MHD system in Elsässer variables, in which the fully discrete solution is obtained by a partitioned iterative non-linear solver at each time step. We proved that the sequence of solutions by the partitioned iteration converges linearly to the solution of the method. We also showed that the proposed method has long-time conservation in the model energy, cross-helicity, magnetic helicity, and is second-order accurate under arbitrary time grids due to the time discretization of the midpoint rule. A time-adaptive algorithm based on the local truncation error criterion was proposed, which balances time efficiency and accuracy. The first two numerical examples confirm the long-time conservation of quadratic Hamiltonians, and the second-order accuracy of the proposed method, while the third stiff test problem demonstrates the advantage of time adaptivity.

REFERENCES

- [1] H. Alfvén. Existence of electromagnetic-hydrodynamic waves. *Nature*, 150:405, 1942.
- [2] U. M. Ascher and S. Reich. The midpoint scheme and variants for Hamiltonian systems: advantages and pitfalls. *SIAM J. Sci. Comput.*, 21(3):1045–1065, 1999.
- [3] L. Barleon, V. Casal, and L. Lenhart. MHD flow in liquid-metal-cooled blankets. *Fusion Eng. Des.*, 14:401 – 412, 1991.
- [4] J. D. Barrow, R. Maartens, and C. G. Tsagas. Cosmology with inhomogeneous magnetic fields. *Phys. Rep.*, 449(6):131–171, 2007.
- [5] P. B. Bochev and C. Scovel. On quadratic invariants and symplectic structure. *BIT*, 34(3):337–345, 1994.
- [6] S. C. Brenner and L. R. Scott. *The mathematical theory of finite element methods*, volume 15 of *Texts in Applied Mathematics*. Springer-Verlag, New York, 1994.
- [7] J. Burkardt, W. Pei, and C. Trenchea. A stress test for the midpoint time-stepping method. *Int. J. Numer. Anal. Model.*, 19(2-3):299–314, 2022.
- [8] J. Burkardt and C. Trenchea. Refactorization of the midpoint rule. *Appl. Math. Lett.*, 107:106438, 2020.
- [9] F. Capuano, B. Sanderse, E. De Angelis, and G. Coppola. A minimum-dissipation time-integration strategy for large-eddy simulation of incompressible turbulent flows. In *AIMETA 2017 Proceedings of the XXIII Conference of the Italian Association of Theoretical and Applied Mechanics*, pages 2311–2323, Sept. 2017.
- [10] P. G. Ciarlet. *The finite element method for elliptic problems*, volume 40 of *Classics in Applied Mathematics*. Society for Industrial and Applied Mathematics (SIAM), Philadelphia, PA, 2002. Reprint of the 1978 original [North-Holland, Amsterdam].
- [11] G. G. Dahlquist, W. Liniger, and O. Nevanlinna. Stability of two-step methods for variable integration steps. *SIAM J. Numer. Anal.*, 20(5):1071–1085, 1983.
- [12] P. A. Davidson. *An introduction to magnetohydrodynamics*. Cambridge Texts in Applied Mathematics. Cambridge University Press, Cambridge, 2001.
- [13] M. Dobrowolny, A. Mangeney, and P. Veltri. Fully developed anisotropic hydromagnetic turbulence in interplanetary space. *Phys. Rev. Lett.*, 45(2):144–147, 1980.
- [14] E. Dormy and M. Núñez. Introduction [Special issue: Magnetohydrodynamics in astrophysics and geophysics]. *Geophys. Astrophys. Fluid Dyn.*, 101(3-4):169, 2007.
- [15] W. M. Elsässer. The hydromagnetic equations. *Phys. Rev.*, 79:183–183, Jul 1950.
- [16] J. A. Font. General relativistic hydrodynamics and magnetohydrodynamics: hyperbolic systems in relativistic astrophysics. In *Hyperbolic problems: theory, numerics, applications*, pages 3–17. Springer, Berlin, 2008.
- [17] G. P. Galdi. *An introduction to the mathematical theory of the Navier-Stokes equations*. Springer Monographs in Mathematics. Springer, New York, second edition, 2011. Steady-state problems.
- [18] S. Galtier, S. V. Nazarenko, A. C. Newell, and A. Pouquet. A weak turbulence theory for incompressible magnetohydrodynamics. *J. Plasma Phys.*, 63:447–488, 6 2000.

- [19] J.-F. Gerbeau, C. Le Bris, and T. Lelièvre. Mathematical methods for the magnetohydrodynamics of liquid metals. Numerical Mathematics and Scientific Computation. Oxford University Press, Oxford, 2006.
- [20] V. Girault and P.-A. Raviart. Finite element methods for Navier-Stokes equations, volume 5 of Springer Series in Computational Mathematics. Springer-Verlag, Berlin, 1986. Theory and algorithms.
- [21] P. Goldreich and S. Sridhar. Toward a theory of interstellar turbulence. II: Strong Alfvénic turbulence. ApJ, 438:763–775, 1995.
- [22] E. Hairer, S. P. Nørsett, and G. Wanner. Solving ordinary differential equations. I, volume 8 of Springer Series in Computational Mathematics. Springer-Verlag, Berlin, second edition, 1993. Nonstiff problems.
- [23] H. Hashizume. Numerical and experimental research to solve MHD problem in liquid blanket system. Fusion Eng. Des., 81:1431 – 1438, 2006.
- [24] J. G. Heywood and R. Rannacher. Finite-element approximation of the nonstationary Navier-Stokes problem. IV. Error analysis for second-order time discretization. SIAM J. Numer. Anal., 27(2):353–384, 1990.
- [25] V. John. Finite element methods for incompressible flow problems, volume 51 of Springer Series in Computational Mathematics. Springer, Cham, 2016.
- [26] R. H. Kraichnan. Inertial-range spectrum of hydromagnetic turbulence. Phys. Fluids, 8(7):1385–1387, 1965.
- [27] W. Layton, W. Pei, Y. Qin, and C. Trenchea. Analysis of the variable step method of Dahlquist, Liniger and Nevanlinna for fluid flow. Numer. Methods Partial Differential Equations, 38(6):1713–1737, 2022.
- [28] W. Layton, W. Pei, and C. Trenchea. Refactorization of a variable step, unconditionally stable method of Dahlquist, Liniger and Nevanlinna. Appl. Math. Lett., 125:Paper No. 107789, 2022.
- [29] W. Layton, W. Pei, and C. Trenchea. Time step adaptivity in the method of Dahlquist, Liniger and Nevanlinna. Advances in Computational Science and Engineering, 1(3):320–350, 2023.
- [30] Y. Li and C. Trenchea. Partitioned second order method for magnetohydrodynamics in Elsässer variables. Discrete Contin. Dyn. Syst. Ser. B, 23(7):2803–2823, 2018.
- [31] T. Lin, J. Gilbert, R. Kossowsky, and P. S. U. S. COLLEGE. Sea-Water Magnetohydrodynamic Propulsion for Next-Generation Undersea Vehicles. Defense Technical Information Center, 1990.
- [32] B. Lindberg. On a dangerous property of methods for stiff differential equations. Nordisk Tidskr. Informationsbehandling (BIT), 14:430–436, 1974.
- [33] W. Pei. The semi-implicit DLN algorithm for the Navier-Stokes equations. Numer. Algorithms, 97(4):1673–1713, 2024.
- [34] W. Pei. The variable time-stepping DLN-ensemble algorithms for incompressible Navier-Stokes equations. arXiv 2407.19101, 2024.
- [35] B. Punsly. Black hole gravitohydromagnetics, volume 355 of Astrophysics and Space Science Library. Springer-Verlag, Berlin, second edition, 2008.
- [36] S. Shehzad, T. Hayat, and A. Alsaedi. Influence of convective heat and mass conditions in MHD flow of nanofluid. Bull. Pol. Acad. Sci. Tech. Sci., 63(2):465–474, 2015.
- [37] F. Siddiqua and W. Pei. Variable time step method of Dahlquist, Liniger and Nevanlinna (DLN) for a corrected Smagorinsky model. Int. J. Numer. Anal. Model., 21(6):879–909, 2024.
- [38] C. Trenchea. Unconditional stability of a partitioned IMEX method for magnetohydrodynamic flows. Appl. Math. Lett., 27:97–100, 2014.
- [39] C. Trenchea. Partitioned conservative, variable step, second-order method for magnetohydrodynamics in Elsässer variables. ROMAI J., 15(2):117–137, 2019.
- [40] N. Wilson, A. Labovsky, and C. Trenchea. High Accuracy Method for Magnetohydrodynamics System in Elsässer Variables. Comput. Methods Appl. Math., 15(1):97–110, 2015.
- [41] G. Yuksel and R. Ingram. Numerical analysis of a finite element, Crank-Nicolson discretization for MHD flows at small magnetic Reynolds numbers. Int. J. Numer. Anal. Model., 10(1):74–98, 2013.